Source Sector and Region Contributions to Black Carbon and PM$_{2.5}$ in the Arctic

Negin Sobhani[1,2], Sarika Kulkarni[2,3], and Gregory R. Carmichael[2]

[1] National Center for Atmospheric Research, Boulder (NCAR), Colorado, USA

[2] Center for Global and Regional Environmental Research (CGRER), University of Iowa, Iowa City, Iowa, USA

[3] California Air Resources Board (CARB), Sacramento, California, USA

Correspondence to: Negin Sobhani (negins@ucar.edu)

Abstract

The impacts of BC and PM$_{2.5}$ emissions from different source sectors (e.g. transportation, power, industry, residential, and biomass burning) and source regions (e.g. Europe, North America, China, Russia, Central Asia, South Asia, and the Middle East) to Arctic BC and PM$_{2.5}$ concentrations are investigated using a series of sensitivity runs with WRF-STEM modeling framework. The simulations are validated using aircraft observations over the Arctic during spring and summer 2008. Emissions from power, industrial, and biomass burning sectors are found to be the main contributors to the Arctic PM$_{2.5}$ with contributions of ~30%, ~25%, and ~20% respectively. In contrast, the residential and transportation sectors are identified as the major contributors to Arctic BC with contributions of ~38% and ~30%. Anthropogenic emissions are the most dominant contributors (~88%) to the BC surface concentration over the Arctic; however, the contribution from biomass burning is significant over the summer (up to ~50%). Among all geographical regions, Europe and China have the highest contributions to the BC surface concentrations with contributions of ~46% and ~25% respectively. Further sensitivity runs show that among various economic sectors of all geographic regions, European and Chinese residential sector contribute up to ~25% and ~14% to the Arctic average surface BC concentration. For Arctic PM2.5, the anthropogenic emissions contribute > ~75% at the surface annually, with contributions of ~25% from Europe and ~20% from China; however, the contributions of biomass burning emissions are

significant in particular during spring and summer. The contributions of each geographical region to the Arctic PM$_{2.5}$ and BC vary significantly with altitude. The simulations show that the BC from China is transported to the Arctic in the mid-troposphere, while, BC from European emission sources are transported near the surface under 5km, especially during winter.

1. Introduction

Arctic temperature has increased more than the mean global surface air temperature over the past century due to various positive feedbacks and amplification mechanisms such as black carbon (BC) deposition and albedo reduction (AMAP, 2011a, 2011b, 2015; Cohen et al., 2012; IPCC, 2013; Screen and Simmonds, 2010). Long-range transport of atmospheric particulate matter (PM) from mid-latitudes to the Arctic is the main contributor to the Arctic aerosol load (AMAP, 2011b; Law and Stohl, 2007; Quinn et al., 2007). Several studies, as early as the 1980s, reported a distinctive seasonal cycle in the Arctic aerosol and BC concentration and visibility (Barrie, 1986; Quinn et al., 2007; Rosen et al., 1981; Schnell, 1984; Wang et al., 2011). The so-called Arctic Haze phenomenon in the winter-spring period has been attributed to increased levels of transported Particulate Matter (PM) from anthropogenic emission sources at lower latitudes and slower wet deposition removal processes (Barrie et al., 1981; Law and Stohl, 2007; Quinn et al., 2002, 2007).

BC is a critical component of the Arctic haze, and influences global climate and water cycles in various ways (AMAP, 2011b; Bond et al., 2013; Shindell et al., 2008). BC particles in the atmosphere absorb solar radiation and warm the surrounding air. When deposited on snow and ice, BC reduces the surface albedo and absorbs more solar radiation; hence, increases the temperature of snow and accelerates the snow melting process (Clarke and Noone, 1985; Flanner et al., 2007; Hansen and Nazarenko, 2004; Koch et al., 2007; Wiscombe and Warren, 1980). Although BC is a minor contributor to aerosol loading (~10%), it has been identified as the second largest contributor to global warming after carbon dioxide (CO$_2$) (Ramanathan and Carmichael, 2008). Studies suggest that BC has caused ~25% of the 20th century warming over the Arctic (Bond and Sun, 2005; Koch and Hansen, 2005; Ramanathan and Carmichael, 2008). Although BC plays a significant role in global climate, there is high uncertainty in assessing the magnitude of BC effects on radiative forcing in climate (Bond et al., 2013; Flanner et al., 2007). Considering the short atmospheric lifetime of BC and its significant impact on the Arctic climate, mitigating BC emissions provides us with an opportunity to decrease BC concentration in the atmosphere immediately to reduce near-term climate impacts (Bond and Sun, 2005; Hansen and Sato, 2001; Jacobson, 2002; Ramanathan and Carmichael, 2008). To devise effective global BC emission abatement policies,

it is necessary to quantify the contribution of each geographical source region and source sector, and to identify the major transport pathways to the Arctic (AMAP, 2011b).

BC in the Arctic has both natural (e.g. biomass burning) and anthropogenic sources (e.g. smelter emissions from Norilsk or the Kola peninsula) (Schmale et al., 2011), but there are very few emission sources

5   locally within the Arctic region (AMAP, 2011b; Law and Stohl, 2007). Hence, the main contributor to BC in the Arctic atmosphere is the long-range transport of particles from mid and high-latitude regions (AMAP, 2011b; Bond et al., 2013; Law et al., 2014; Law and Stohl, 2007). Several studies have shown that transport of aerosols from mid-latitudes is the most significant transport mechanism to the Arctic pollution (AMAP, 2011b; Law and Stohl, 2007). Previous studies in literature have identified Europe as the major source region contributor to Arctic

10   BC concentrations (Barrie, 1986; Quinn et al., 2007, 2008; Raatz and Shaw, 1984; Shaw, 1995). However, during the past two decades emissions from East Asia have increased rapidly due to the vast economic growth, while the emissions from Europe have declined during the same time period (Streets et al., 2009). Recent studies have shown the significant contribution of Asian emissions to the Arctic, especially during winter-spring (Breider et al., 2014; Fisher et al., 2010; Koch and Hansen, 2005; Shindell et al., 2008; Stohl, 2006; Wang et al., 2011).

15   However, there is significant uncertainty associated with these estimates (Fisher et al., 2010; Koch and Hansen, 2005; Sharma et al., 2013b; Stohl et al., 2006; Wang et al., 2011). There are number of factors including but not limited to the uncertainties in emissions, and the complicated transport pathways from mid-latitudes to the Arctic that contribute to the uncertainties in calculating the impacts of emission sources (Bian et al., 2013; Fuelberg et al., 2010).

20   Modeling BC concentrations over the Arctic is considered a challenging task for chemical transport models (Eckhardt et al., 2015; Koch et al., 2009; Shindell et al., 2008; Wang et al., 2011). Previous model inter-comparison studies have shown order of magnitude differences between observation and model (Bond and Sun, 2005; Wang et al., 2011). The studies by Shindell et al., 2008 and Koch et al., 2009 have shown negative bias between model and observation. However, Shwartz et al. (2010) shows positive bias comparing global models with observation (Shwartz et al. 2010, Sharma et al., 2013). These differences between model performances are

25   largely due to the high uncertainty in emissions and scavenging efficiency for calculating wet deposition (Bourgeois and Bey, 2011; Liu et al., 2015). Regional chemical transport models with a focus on the Arctic capture the BC concentration better over the Arctic. Koch et al. 2009 and Liu et al., 2011 studies captured the NASA ARCTAS flights vertical profiles and seasonality well.

In this study, we designed a modeling framework (WRF-STEM) for analyzing BC, organic carbon (OC), SO_4, $PM_{2.5}$, and PM_{10} concentrations over the Arctic. We utilize this system to study the seasonal variations in the contributions of emissions from different source sectors (e.g. transportation, power, industry, residential, and biomass burning) and source regions (e.g. Europe, North America, China, Russia, Central Asia, South Asia, and the Middle East) on Arctic PM mass concentration (Figure SM1). Section 2 describes the data sources and modeling framework utilized in this study, while the findings are discussed in section 3 followed by conclusions in section 4.

2. Method and Data

2.1. Modeling System

2.1.1. Meteorological Model

The Weather Research and Forecasting model (WRF) version 3.4 was used for producing necessary meteorological inputs for the STEM model. The ice sheet coverage, initial and boundary conditions for the model were provided by the National Center for Environmental Prediction (NCEP) Final Analysis (FNL, http://rda.ucar.edu/datasets/ds083.2/). The meteorological factors affecting chemical distribution and concentration were imported into the STEM model every 6 hours as described in Kulkarni et al., 2015.

2.1.2. Emissions

The base emission setup used for this modeling study is similar to Kulkarni et al. 2015, except that anthropogenic emissions were updated to the HTAP_v2.2 for year 2008 (Janssens-Maenhout et al., 2015). A new source category of emissions from open waste burning from Wiedinmyer et al., 2014 were also utilized in this study. For carbonaceous aerosols and PM emissions from biomass burning sector, FINNv1 from Wiedinmyer et al., 2011 was used. Dust emissions were estimated using Uno et al., 2004 method for grids with snow cover <1%. Further details of the biomass burning and dust emissions described in Kulkarni et al. 2015 and Sobhani, 2017.

Figure 1 shows the regional distribution of anthropogenic and wildfire BC emissions for the modeling domain. The major anthropogenic BC emission hotspots are over China and India along with significant emissions from Eastern Contiguous United States (CONUS), Europe, and Northern Middle East regions. The major hotspots of wild fire BC emissions are over South East Asia, Siberia, and Europe. There are also wild fire emission sources from Southeastern and Western CONUS (Figure 1).

Figure 2 shows the anthropogenic BC emissions from the different economic sectors. The residential source sectors is the major source of BC emissions over Asia (including China, India, and Southeastern Asia) with values ranging from ~45% to ~95% of total anthropogenic BC emissions. The transportation sector is the dominant emission sector over North America and Central Asia with values ranging from 35% to 90%. The Industry sector contributes between ~35% to ~50% of total BC emissions over Central Asia and Siberia.

2.1.3. Chemical Transport Model

The WRF-STEM modeling framework is similar to that used by Kulkarni et al. 2015 except for updated anthropogenic emissions (described above). The STEM model is a regional scale Chemical Transport Model (CTM) developed at the University of Iowa in the 1980's and has continuously developed since then. The STEM model includes the emission, transport (convective and diffusive), and deposition of particles and chemicals based on Eulerian approach.

The modeling domain for both WRF and STEM models covers most of the Northern hemisphere including the significant emission sources such as Asia, Russia, Europe and North America. Also, the model extends over the Northern Africa, Middle East, and South Asia to include the dust emissions from the arid regions and anthropogenic emissions from the population-dense regions. The model used polar stereographic map projection with 60 km horizontal resolution (249x249 grid cells). This modeling system is described in further details in Kulkarni et al., 2015 and D'Allura et al., 2011.

2.2. Observations

For evaluating the modeling system performance, the model's outputs were compared with aircraft data from the National Aeronautics and Space Administration (NASA) Arctic Research of the Composition of the Troposphere from Aircraft and Satellites (ARCTAS) field campaign (Jacob et al., 2010). The ARCTAS field campaign measurements included observations from DC-8, P-3 and B-2000 research aircraft and data analysis and forecasts by different global and regional modeling teams. The ARCTAS field campaign took place as a part of the international POLARCAT framework (POLar study using Aircraft, Remote sensing, surface measurements and models, of Climate, chemistry, Aerosols, and Transport; see Law et al., 2014 , and www.polarcat.no) during the 2007-2008 international polar year, with the goal to better understand the factors causing changes in the Arctic atmospheric composition and radiative forcing (Jacob et al., 2010; Law et al., 2014). The spring phase (ARCTAS-A) which happened during April 2008, was concurrent with an unusually higher number of Siberian fires, which subsequently caused higher concentrations of carbonaceous aerosols (Fuelberg et al., 2010; Jacob et

al., 2010; Kondo et al., 2011; Liu et al., 2015; Matsui et al., 2011; McNaughton et al., 2011; Spackman et al., 2010; Wang et al., 2011; Warneke et al., 2009). Figure SM2 panels show the flight pathways of all ARCTAS flights during spring (ARCTAS-A) and summer 2008 (ARCTAS-B) respectively.

5   The model performance was evaluated during different seasons by comparing simulated concentrations with the surface observations at two sites located in the Arctic: Barrow Alaska (156.6° W, 71.3° N, 11 m a.s.l.) and Alert (Nunavut), Canada (62.3° W 82.5° N, 210 m a.s.l.) depicted in Figure SM2. The Barrow site is located northeast of the Barrow town at the northern edge of Alaska. Observations at Barrow are retrieved from National Oceanic and Atmospheric Administration (NOAA) Global Monitoring Division (GMD), where a particle soot absorption photometer (PSAP) is used for measuring BC light absorbing coefficient at three wavelengths (476,

10   530, and 660 nm) (Bodhaine, 1989; Bond et al., 1999; Delene and Ogren, 2002 ; Data is available at https://esrl.noaa.gov/gmd/aero/net/). The Alert station, located in the northernmost Qikiqtaaluk region of Canada, is mostly isolated from both local and continental source regions. The Alert observatory is the most northerly site of World Meteorological Organization (WMO) Global Atmosphere Watch (GAW) network. Alert BC concentrations are calculated using light absorption coefficient data measured by Environment and Climate

15   Change Canada using a PSAP (Radiance Research, Inc.) at three wavelengths (476, 530, and 660 nm) (Sharma et al., 2004, 2013a, 2017; Data is available at http://ebas.nilu.no/). The light absorption coefficients are converted to Equivalent Black Carbon (EBC) using mass absorption cross-section (MAC). In this study for calculating EBC concentration, light absorption coefficient at 530nm was used with a MAC value of 9.5 m^2/g as recommended by (Qi et al., 2017a; Sharma et al., 2013b; Stohl et al., 2013).

20   For further validating the model's performance outside the Arctic's circle, BC surface concentration data was evaluated using annual average data from 168 Interagency Monitoring of Protected Visual Environment (IMPROVE) sites over North America and is described in section 3.1.2.

3. Results and Discussions

3.1. Model Evaluation

25   #### 3.1.1. Meteorological Model Evaluation
The spring and summer 2008 ARCTAS flight tracks are illustrated in Figure SM2 a and b respectively. To evaluate performance of the model for different regions in the Arctic, the flights were categorized into the

following 7 categories based on the location and time of the flights including, 1- spring Alaska local flights, 2-spring Greenland flights, 3-spring transit flights, 4- summer California flights, 5- summer Canada local flights, 6-summer Canada Greenland flights, and 7- summer transit flights. Table 1 shows the different flight categories and the date of the flights corresponding to each category. The model data were evaluated for each individual flight and each flight category.

Figure 3 boxplots compare the model vs. observation meteorological data for each of the flights. Each flight category is shaded with a different color and the spring and summer transition flights are not shaded. The simulated meteorological variables were extracted along the DC-8 flight pathways and compared against observational data measured on the DC-8. For each of the flights, simulation and measured data, combined at all altitudes, were summarized into one separate box/whisker plot. Table 2 shows statistical summary of comparison between modeled and measured metrological parameters.

These results and further analysis by altitude (Figure SM4) show that the modeled meteorology captured the many of the observed features seen in temperature, Relative Humidity (RH), and wind speed. Temperature shows a slight positive bias for summer flights and a negative bias at higher altitudes during spring. In addition, the model under-predicts RH during the spring and summer California flights, while it over-predicted it during the summer Canada Greenland flights. The RH under-prediction happens at lower latitudes for spring flights and over-prediction occurs in higher altitudes for summer flights. The model also tends to slightly over-predict wind speed by (~4%) at higher altitudes during spring flights. The model under-predicted the wind speed for all summer California flights. The model captured the RH vertical distribution in the lower troposphere but displays a large negative bias at altitudes above ~4km. This indicates the difficulties in capturing the complex ice and cloud formation properties at high altitudes in the polar region during springtime.

Table 2 summarizes the statistical summary of the major meteorological variables for both ARCTAS observation data and model output. Based on this table and box and whisker plots analysis the model captures vertical profiles and magnitudes of meteorological observations from ARCTAS.

3.1.2. Concentration Evaluation

Concentration Evaluation along ARCTAS DC-8 flights

The simulated air pollution concentrations were evaluated using NASA ARCTAS flight data. Table 1 shows the NASA ARCTAS flight categories and Figure SM2 panels show the flight tracks for spring and

summer. Figure 4 shows boxplots comparing concentrations of BC, SO_4, and SO_2 for model and observations for each ARCTAS flight. The flight categories are shaded similar to Figure 3. The results show that generally, simulated BC follows the same flight-by-flight variation as observed with an overall high bias (Figure 4).

Figure 5 compares the vertical BC and SO_4 concertation profiles for all flights. The vertical profiles for each flight category are shown in Figure SM3. In the vertical profile plots, both modeled and observed values are binned by flight altitudes every 1 km. The model captured the vertical variability of BC and SO_4 concentration well (Figure 5). For BC, both observation and model show the highest values near the surface. The simulated BC values are biased high above 5 km for all flight categories (Figure SM3). There is also a constant over-prediction of SO_4 above 5km, which may be due in part to an under-prediction of RH, resulting in under-estimation of wet removal and in-cloud scavenging at altitudes above 5km.

BC Surface Concentration Evaluation at Barrow and Alert

For evaluating the model performance in capturing the seasonality of BC concentration in the Arctic region, we compared the simulated BC surface concentrations with BC data available at Barrow and Alert stations for the duration of study (April 2008- March 2009). When using EBC values, it is very important to keep in mind that the MAC values used for estimating EBC has a large range (from $5m^2/g$ to 20 m^2/g) and EBC concentrations has at least a factor of two uncertainty (Bond and Bergstrom, 2006; Liousse et al., 1996; Sharma et al., 2002, 2017; Weingartner et al., 2003). Traditionally, a MAC value of 10 m^2/g was used for EBC calculations for aged BC particles and Sharma et al., 2013a used MAC values of 19 m^2/g for both Barrow and Alert sites. However, recent studies suggest much lower values for MAC compared to the 9.5 m^2/g used for this study. Sharma et al., 2017 suggest MAC values of 5 ±2 m^2/g for summer-time and Sinha et al., 2017 suggested MAC values as low as 8.5 m^2/g for Barrow site. Using the lower values of MAC values, will result in higher observed EBC.

Figure 6 shows the time-series boxplots of simulated BC vs. observed EBC concentration for the duration of the study at the surface for the Alert and Barrow sites. The model accurately predicted the seasonality of BC in both sites. Both model and observation show higher values of BC during winter and spring, indicating the Arctic Haze. At the Alert site, the model especially captured the wintertime and springtime peak values; however, it over-predicted the summer BC concentration. Using lower MAC values as suggested by Sharma et al., 2017 for summertime results in 1.9x higher observed EBC which will be closer to the simulated values.

For the Barrow site, the model consistently over-estimates the BC concentrations during the year. The over-estimation of BC during summer can be due to the large contributions of biomass burning from Siberia in the simulations caused by overestimations of emissions and/or too little removal during transport. However, Stohl, 2006 and Stohl et al., 2013 studies discussed that the biomass burning contributions from remote locations were unintentionally removed in the Barrow measurements data processing. By removing the data cleaning for Barrow site, the observations were increased by a factor of 2-3 during summer.

BC Concentration Evaluation for IMPROVE sites

The simulated air pollution concentrations were further evaluated using data from 168 IMPROVE sites over the U.S. for the period of April 2008 to July 2009 (Data available from http://vista.cira.colostate.edu/improve/Data/IMPROVE/AsciiData.-asp). Figure 7 shows the annual mean surface BC concentration over the U.S. compared with observations at IMPROVE network sites. Each site is represented as a circle in the map. The average model BC over the U.S. is 0.16 $\mu g/m^3$ while average IMPROVE data is 0.19 $\mu g/m^3$. Further statistical analysis shows that the root-mean-square deviation (RMSE) between model and observation is 32% and the mean bias error (MBE) is 0.03 $\mu g/m^3$.

3.2. Spatial Distribution of PM Species

BC and SO_4 are major parts of $PM_{2.5}$, and can be transported over long distances and across the continents, and they both have various anthropogenic and natural emission sources. Figure 8 shows the annual average concentrations of surface BC, SO_4, $PM_{2.5}$, and PM Ratio over the entire modeling domain. Figure 8-a shows that the modeled BC surface concentration is in the range of ~0.25 to 3 $\mu g/m^3$. The major BC hotspots are over Southeast Asia, northern India, and China with annual average concentrations of ~3 $\mu g/m^3$. Furthermore, the seasonal and monthly results show that BC concentration peaks during wintertime since there are higher biomass and fossil fuel burning for heating during the winter season. The annual average surface concentration over the U.S. is 0.16 $\mu g/m^3$ with the maximum BC over the Eastern U.S. with average of 0.75 $\mu g/m^3$. The annual average BC for the Arctic area (latitudes > 60°N) is between ~0.025 $\mu g/m^3$–0.075$\mu g/m^3$ with the minimum occurring over Greenland, Alaska and Northern Canada. This value is consistent with the average of 0.06$\mu g/m3$ over the Arctic from Sharma et al. 2013-b.

SO_4 can be produced by sea spray or volcanos, but they are mostly from oxidation of SO_2 emitted during combustion of sulfur-containing fossil-fuels (IPCC, 2007). SO_4 scatters solar radiation and has a negative direct

radiative forcing. Figure 8-b shows that the major SO_4 levels are in Asia and northern India, with less intense but significant concentrations over Europe and eastern CONUS. The concentration of SO_4 particles over East Asia is approximately two times higher than SO_4 concentration over the eastern CONUS and Europe. This is due to higher SO_2 emissions in the Asian region and relatively faster SO_2 oxidation rates (Chin et al., 2007).

5   Figure 8-c shows the distribution of surface $PM_{2.5}$. Major $PM_{2.5}$ hotspots are over the Persian Gulf, Central Asia, northern India and northern Africa with annual average maxima as high as ~80 $\mu g/m^3$ around the Persian Gulf. The Arctic area (above 60°N) show values between 1- 5 $\mu g/m^3$ with maximum occurring over northern Europe and northern Russia. Greenland, Northern Canada and Alaska show average $PM_{2.5}$ concentrations of ~2 $\mu g/m^3$. Figure 8-d shows the $PM_{2.5}/PM_{10}$ ratio, which is an indicator of relative contributions

10   from anthropogenic and natural sources. The arid regions with high natural dust emissions such as northern African, the Persian Gulf, and Central Asia show lower PM ratios indicating the major contributions of dust to PM over these regions. Over the oceans, the PM ratio is very low (0.1-0.2) caused by higher contributions of sea salt to PM_{10} and low $PM_{2.5}$ concentration (~84% contribution of coarse sea salt to PM 10 over the Atlantic Ocean and ~75% over the Pacific Ocean). Higher PM ratio values in eastern Asia and eastern CONUS indicate that the

15   sources of PM in these regions are mostly anthropogenic.

3.3. Sources of Arctic PM

3.3.1. Source sectors contributing to PM surface concentration

Due to the significant contribution of BC in global warming over the Arctic, it is important to understand the influence of specific source regions and source sectors on the Arctic BC concentration. Figure 9 shows the 5

20   major source sector contributions percentage to BC surface concentrations. Transportation is the major sector contributor over North America with contributions ranging from ~30% to ~55%. The residential sector is the major contributor to BC over China and South Asia with maximum residential contribution percentage as high as ~70 %, which is generally consistent with spatial pattern of emissions (Figure 2). However, the residential sector has a significant (~25%) contribution over Western U.S. reflecting the outflow of Asian BC over Pacific Ocean

25   and to the West Coast. The residential, transportation and industrial sectors are the major emission sources over Europe as shown in figure 2. Over the Arctic (60 °N and above) residential and transportation sectors show maximum contributions of ~38% and ~30%, respectively. The contribution from the biomass burning sector over the Siberian Arctic is substantial with values as high as ~40% , which can be attributed to the large number of forest fires particularly during springtime. Industrial and power emissions had the highest contributions on the

Arctic SO_4 concentration, while biomass burning, power and industrial emissions have the highest contributions to Arctic $PM_{2.5}$ (Figure SM 5 and SM 6 respectively). Figure SM 5 shows the large contributions of power sector to Europe SO_4 and high contributions industrial sector over North America and Siberia. Based on Figure SM 6, power sector is the major contributor to $PM_{2.5}$ over the Europe and eastern US, and Industrial sector is the most

5   significant contributor to $PM_{2.5}$ over Canada, western US, Russia, and China. Biomass burning has significant contributions to $PM_{2.5}$ over southeastern Asia, Western US, and Russia. Residential sector has high impact on Eastern China and Indo-Gangetic plain $PM_{2.5}$ surface concentration based on Figure SM 6.

The seasonality of sector contributions to the Arctic pollution is shown in Figure 10. Figure 10- top panel shows the time series contribution from five emission sectors to BC surface concentration over the Arctic. For

10   this plot, the area average surface concentration for latitudes 60°N and above is shown.   The surface concentrations range from 0.05 µg/m^3 to 0.2 µg/m^3 over the Arctic. The maximum BC concentrations occur during wintertime, indicating the prevalence of Arctic haze. The contribution from residential sector significantly increases during wintertime, since burning of biofuels and coal are the main heating resource at higher latitudes. Furthermore, there is a high seasonal variability in the contribution of biomass burning with maximum values

15   occurring during the springtime due to the widespread seasonal agricultural burning over Russia and the increased occurrence of Siberian forest fires (AMAP, 2011b). During spring 2008, biomass burning was reported to be unusually high (AMAP, 2011b; Jacob et al., 2010; Liu et al., 2015; Matsui et al., 2011; Wang et al., 2011; Warneke et al., 2009). Furthermore, during the spring the arctic front is more southerly on the Eurasian side (Bond et al., 2013; Stohl, 2006). Hence, the BC emitted from agricultural burning and boreal forests from Europe

20   and Russia transport easily, especially at lower altitudes. These results are similar to Qi et al., 2017b , Brock et al., 2011, Warneke et al., 2010, and Bond et al., 2013 , which suggest that high-latitude agricultural and boreal forest fire is one of the main contributors to BC over the Arctic during spring 2008.

The middle panel of Figure 10   shows the time series of contributions from the emission sectors to anthropogenic $PM_{2.5}$ and biomass burning over the Arctic. Biomass burning contributes to the $PM_{2.5}$ seasonality

25   with maximum contribution in spring and summer. The power, industry, and transportation sectors are the highest contributors during wintertime, reflecting the increased energy consumption for both domestic and industrial heating.

Figure 10- bottom panel shows the contribution of different $PM_{2.5}$ components to the Arctic total $PM_{2.5}$ concentration. BC comprises an average of ~5% of $PM_{2.5}$ over the Arctic. Fine dust (defined as dust with

aerodynamic diameter of less than 2.5 μm) is a major source of $PM_{2.5}$ seasonal variation, with maximum contribution in spring (~40%). SO_4 shows the highest contribution over the winter months with a peak of ~60%. SO_4 maximum in winter is caused by the shift in the transport pathways of pollutants during wintertime over the Europe. The high values of SO_4 during the cold months are mostly caused by the large Europe contribution with

5   higher use of fossil fuel and coal burning and SO_2 emissions for industry, power and residential purposes. The industry and power sectors have the highest contributions to the Arctic SO_4 concentration (each ~42%) on an annual basis. The transport pathways and seasonality are further described in the transport pathways section.

3.3.2. Geographical source contribution to PM concentration

Contributions of BC emissions from different source regions (i.e. Europe, China, North America, Central

10   Asia, Middle East, South Asia, Central Asia and Siberia) were also analyzed using sensitivity analysis. Figure 11 shows the spatial plots of annual average contributions from different geographical regions to BC surface concentration. Europe and China have the largest contribution to BC surface concentration over the Arctic. China contributes to ~35% of the BC in Canada, Northwestern CONUS and Alaskan regions, which indicates the significant of the inter-continental transport of BC. North American BC emissions have up to ~20% contribution

15   to Southern Europe surface BC concentration.

The source region contributions to surface and column BC concentration also show seasonal variability. Figure 12 shows the contributions of different emission regions to BC surface concentration and column amounts. Anthropogenic emissions from Europe and China have the highest impact on the Arctic surface BC concentration with annual averages of ~46% and ~25%. However, Europe only contributes to ~25% of the Arctic

20   BC column and China contributes ~36% of column BC in the Arctic. During the winter and spring, air masses from colder and drier regions can follow surfaces of constant potential temperature and cross the Arctic front barrier but emissions from moister and warmer regions such as North American and China cannot easily cross the Arctic front. However, these particles originating from warmer and moister regions can be lifted and transported to the Arctic in the middle and upper troposphere along the isentropes (AMAP, 2011b; Barrie, 1986; Law and

25   Stohl, 2007; Stohl, 2006). Therefore, emissions from northern latitudes such as (Europe and Russia) have higher contributions to the surface concentration but emissions from lower latitudes have higher contributions to the column aerosol load. Anthropogenic emissions from North America (Canada and United States) are also significant contributors to the BC column concentration with contributions of ~10%. However, anthropogenic emissions from North America contribute only ~4% of surface concentration over the Arctic. North American

30   emissions are mostly from lower latitudes with higher potential temperature and higher humidity. The major

transport pathway of North American emissions to the Arctic follows constant potential temperatures, which cause cloud formation and precipitation, hence higher wet scavenging of aerosols. Brock et al., 2011, McConnell, 2007, Stohl, 2006, Breider et al., 2014 and Liu et al., 2015 show similar low contributions of North American Anthropogenic emission to the Arctic surface concentration. Less than 5% percent of emissions are transported from each of South Asia and the Middle East to the Arctic. During the winter, anthropogenic emissions from Russia accounts for ~12% of BC surface concentration and less than 5% of column BC concentration over the Arctic. This is due to the thermally stable condition and lower vertical mixing during the winter over Russia. During the spring time, anthropogenic emissions from Europe, China, and Russia account for ~35%, ~25%, and, <~10% of BC surface concentration. This finding is consistent with the study of Koch and Hansen 2005, which showed that emissions from Russia, Europe and South Asia have contributions of 20-30% during springtime.

The peak BC surface concentration occurs during the wintertime; however, the contribution of biomass burning in Siberia significantly increases during spring and summer periods, when the biomass burning emissions are the highest. The contributions of Siberian biomass burning to the Arctic surface and column concentration almost doubled during spring 2008 compared to spring 2009. The spring 2008 peak concentrations are explained in the model by Siberian biomass burning plumes transported to the Arctic with low wet scavenging by precipitation and dilution. During the winter, anthropogenic emissions are accountable for ~97% of BC concentration over the Arctic, while during the summer biomass burning contributes up to ~50% of Arctic BC concentration. During the summer, the contributions of European biomass burning increase. The simulation results also show that the biomass burning plumes from South East Asia can reach the Arctic troposphere accounting for up to ~10% of BC aerosol loading during April 2009.

Figure 13 shows the percentage contributions of various sectors and regions to BC, SO_4, and $PM_{2.5}$ at Alert, Barrow, and the Arctic region average (i.e 60° N and above). This figure shows that the major sector contributors to SO_4 are power and industry at both Alert and Barrow and in the Arctic region. The major region contributors for SO_4 are China and Europe. The sectoral contributions for SO_4 and $PM_{2.5}$ for Barrow are similar to those for the Artic mean. Therefore, Barrow is representative of the sectoral contributions to the Arctic mean SO_4 and $PM_{2.5}$. The geographical contributions show more variability between sites and the Arctic mean. However, the geographical contributions to the BC in Alert is a good representation of that of the Arctic average.

For informing more efficient policies, it is essential to study the impact of emissions from various economic sectors of specific source regions on the Arctic surface and column concentrations. Since Europe and

China had the highest contributions to the Arctic BC concentrations, the impacts of each specific economic sectors from China and Europe on the Arctic PM concentrations were studied further. Figure 13 also shows the annual average concentrations of each economic sector from Europe and China to surface BC concentration. The emissions originating from the residential sector in China contributes ~14% of total BC surface concentration. The residential sector accounts for more than ~55% of total China contribution to the Arctic surface BC concentration. The emissions originating from residential and transportation sectors in Europe account for ~90% (~55% from residential and ~35% from transportation sectors) of total European contributions to the Arctic surface BC.

Figure 12 shows how the contributions of specific emission sectors for China and Europe vary by season. The emissions from European residential sector contributes to ~25% of Arctic BC surface concentration on an annual basis. This impact is much higher during the winter and spring due to higher emissions for heating purposes. Figure 13 (g-l) plots show the contributions of different economic sectors from China and Europe to the impact of emissions from Europe or China to annual surface BC, SO_4, and $PM_{2.5}$ concentrations for Alert, Barrow, and the Arctic average. Emissions from Chinese industry sector and European power sector contribute ~12% and ~18% of the Arctic surface SO_4 concentration. Emissions originating from power, industry and residential sectors in Europe account for ~12%, ~8%, and ~8% of total $PM_{2.5}$ surface concentration over the Arctic respectively. Further seasonal and spatial analysis (Figure SM7 and SM8) show that Chinese residential emissions have higher impacts (up to ~35%) on the Pacific Arctic (including Siberia, Alaska, Canadian sub-arctic, and Bering Sea) during the winter. Further details on the seasonality of contributions of various emission sectors from Europe or China to the BC surface concentrations over the entire domain are presented in Figure SM8 and Figure SM9.

3.4. Long Range Transport Pathways

To further understand the seasonality and transport pathways of BC in the Arctic, the seasonally averaged altitude- latitude cross-sections are shown at 65 °N (entrance boundary for the Arctic) in Figure 14. During the spring, the magnitude of BC is relatively high in Eurasia and Siberia. This is partly due to southerly extent of the polar dome during spring especially over Eurasia, which facilitates the transport of BC emission from lower latitudes to the Arctic. During spring, there are extensive agricultural fires and high number of forest fires in Northern Siberia. In addition, spring 2008 had exceptionally higher numbers (almost double) of Siberian boreal forest fires compared to other years (Liu et al., 2015).

During winter (Figure 14-d), we see higher concentration of BC up to 5km indicating the higher low-level transport of BC from the source regions including North America, Europe and Siberia. This shows the stable and low vertical mixing. During the cold months, Europe is the major contributor to the BC concentration, at lower altitudes as shown in Figure 14-i. This is due to thermally stable conditions over winter, which inhibits the upward transport and vertical mixing of emission plumes. However, China shows higher contribution at mid and upper troposphere, which indicates the transport pathways of Asian plumes to the Arctic (Figure 14-h). The contribution of biomass burning to BC concentration is high during summer over Eurasian Arctic, Siberia, and North American Arctic. The contribution of biomass burning is especially high in spring over Siberia during spring 2008 relative to the other years. Also, higher residential emissions of BC in Europe and Asia during the winter is another factor contributing to the higher BC concentration over the Arctic. Siberian forest fires are the major cause of higher BC concentration in Siberian Arctic during summer (Figure 14-n). The higher rate of wet scavenging during summer causes lower transport via low-level pathways. However, the convection caused by forest fires can inject BC in the free troposphere, which reduces the wet and dry deposition for that plume. Figure 14 (q-t) shows the dust concentration at the 65 °N cross-section. During spring, we have higher altitude plumes of dust transporting to the Arctic. Dust emission sources are usually from lower latitudes dry and semi-arid regions; hence dust transport to the Arctic is usually higher in the troposphere. Summer also shows similar pattern but with less intensity compared to the spring.

4. Conclusions and Future Works

In this study, we used a chemical transport model (STEM) to investigate long-range transport of PM to the Arctic and calculate the contributions of various anthropogenic and biomass-burning emission sources to the Arctic surface and column PM concentrations. The focus of this study was to quantify the source sector and source region contributions to the Arctic aerosols.

This study found that emissions originating from residential and transportation sectors were the major contributors to the Arctic BC loading on an annual basis with contributions of ~38% and ~30% respectively. However, the results showed that power industrial, and biomass burning emissions were the major contributor to the Arctic $PM_{2.5}$ (contributions of ~30%, ~25%, and ~20% respectively). Our simulations showed a distinct seasonality for the contributions of sectors and regions to BC and $PM_{2.5}$ concentration over the Arctic. During the winter peak concentration period, the contributions from residential sector were maximized due to high-energy consumption for heating purposes. Biomass burning also showed a distinct cycle with contributions to BC

surface concertation as high as ~50% during summer and less than ~3% during winter. The contributions of anthropogenic sources to BC concentrations near the surface were dominant varying from ~50% -~97% over the year.   However, the contributions of biomass burning from Siberia were significant during spring (up to 40%), and the contributions of biomass burning emissions from Europe became significant over the summer accounting

5   for up to ~20% of Arctic BC column concentration.

Dust was shown to be one of the most important drivers of Arctic $PM_{2.5}$ seasonality. Dust was the largest component of $PM_{2.5}$ in the region in all seasons except for cold months, when sulfate was the largest contributor to the $PM_{2.5}$.

In this study, we found that the major source regions contributing to BC surface concentrations are

10   Europe and China annually with contributions ~46% and ~25% respectively. Among the various economic sectors from each of the geographic regions, the residential sector from Europe and China were the largest contributors to Arctic BC with ~25% and ~14% respectively. In addition, the contribution of each geographical regions varied significantly by altitude. In the mid and upper troposphere, the contributions of Chinese emissions were higher due to their dominant transport pathway to the Arctic. Model results showed a distinctive temporal

15   variability for regional contributions to the Arctic. In general, the anthropogenic emissions from Europe were the most significant due to its large contributions over the winter (haze season).

There are a number of factors (including but not limited to uncertainites in transport pathways, emission inventories, and removal parametrizations) that can contribute to uncertainties associated with the contributions of each source sector and source regions to the Arctic PM loading. Future Arctic warming, sea ice decline, and

20   industrial development facilitates international shipping and transport via the northern sea route, which consequently increase the Arctic pollutants burden (Law et al., 2017; Marelle et al., 2016). Additional observations at Arctic locations along with higher resolution modeling studies are necessary to reduce these uncertainties in future.

Acknowledgements

25   The University of Iowa group activities are funded by NASA awards (NNX08H56G and NNX12AB78G) and an EPA award (RD-83503701-0). The authors would like to acknowledge ARCTAS science team. We would also like to thank the Global Monitoring Division (GMD) at NOAA Earth System Research Laboratory (ESRL), and Environment and Climate Change Canada for maintaining and providing BC

measurements. We would like to acknowledge World Meteorological Organization (WMO) Global Atmosphere Watch (GAW) and the Norwegian Institute for Air Research (NILU) for hosting the measurement data (http://ebas.nilu.no). We also would like to thank the Emissions Database for Global Atmospheric Research (EDGAR) for developing HTAP emission inventories. The authors would like to thank Christine Wiedinmyer

5   for providing open burning emission data. The authors would like to thank Interagency Monitoring of Protected Visual Environments (IMPROVE) for providing observational data over the CONUS. IMPROVE is a collaborative association of state, tribal, and federal agencies, and international partners. US Environmental Protection Agency is the primary funding source, with contracting and research support from the National Park Service. The Air Quality Group at the University of California, Davis is the central analytical laboratory, with ion

10   analysis provided by Research Triangle Institute, and carbon analysis provided by Desert Research Institute.

References

AMAP: Arctic Climate Issues 2011: Changes in Arctic Snow, Water, Ice and Permafrost, Oslo, Norway., 2011a.

AMAP: The Impact of Black Carbon on Arctic Climate. By: P.K. Quinn, A. Stohl, A. Arneth,T. Berntsen, J. F. Burkhart, J. Christensen, M. Flanner, K. Kupiainen, H. Lihavainen, M. Shepherd, V. Shevchenko,H. Skov, and V. Vestreng., Arctic Monitoring and Assessment Programme (AMAP), Oslo, Norway., 2011b.

AMAP: AMAP assessment 2015: Black carbon and ozone as Arctic climate forcers, Oslo, Norway., 2015.

Barrie, L. A.: Arctic air pollution: an overview of current knowledge, Atmos. Environ., 20(4), 643–663, 1986.

Barrie, L. A., Hoff, R. M. and Daggupaty, S. M.: The influence of mid-latitudinal pollution sources on haze in the Canadian arctic, Atmos. Environ., 15(8), 1407–1419, doi:https://doi.org/10.1016/0004-6981(81)90347-4, 1981.

Bian, H., Colarco, P. R., Chin, M., Chen, G., Rodriguez, J. M., Liang, Q., Blake, D., Chu, D. A., da Silva, A., Darmenov, A. S., Diskin, G., Fuelberg, H. E., Huey, G., Kondo, Y., Nielsen, J. E., Pan, X. and Wisthaler, A.: Source attributions of pollution to the Western Arctic during the NASA ARCTAS field campaign, Atmos. Chem. Phys., 13(9), 4707–4721, doi:10.5194/acp-13-4707-2013, 2013.

Bodhaine, B. A.: Barrow surface aerosol: 1976–1986, Atmos. Environ., 23(11), 2357–2369, doi:https://doi.org/10.1016/0004-6981(89)90249-7, 1989.

Bond, T. C. and Bergstrom, R. W.: Light absorption by carbonaceous particles: An investigative review, Aerosol Sci. Technol., 40(1), 27–67, 2006.

Bond, T. C. and Sun, H.: Can reducing black carbon emissions counteract global warming?, Environ. Sci. Technol., 39(217), 5921–5926 [online] Available from: http://pubs.acs.org/doi/abs/10.1021/es0480421 (Accessed 2 February 2015), 2005.

Bond, T. C., Anderson, T. L. and Campbell, D.: Calibration and Intercomparison of Filter-Based Measurements of Visible Light Absorption by Aerosols, Aerosol Sci. Technol., 30(6), 582–600, doi:10.1080/027868299304435, 1999.

Bond, T. C., Doherty, S. J., Fahey, D. W., Forster, P. M., Berntsen, T., DeAngelo, B. J., Flanner, M. G., Ghan, S., Kärcher, B., Koch, D., Kinne, S., Kondo, Y., Quinn, P. K., Sarofim, M. C., Schultz, M. G., Schulz, M., Venkataraman, C., Zhang, H., Zhang, S., Bellouin, N., Guttikunda, S. K., Hopke, P. K., Jacobson, M. Z., Kaiser, J. W., Klimont, Z., Lohmann, U., Schwarz, J. P., Shindell, D., Storelvmo, T., Warren, S. G. and Zender, C. S.: Bounding the role of black carbon in the climate system: A scientific assessment, J. Geophys. Res. Atmos., 118(11), 5380–5552, doi:10.1002/jgrd.50171, 2013.

Bourgeois, Q. and Bey, I.: Pollution transport efficiency toward the Arctic: Sensitivity to aerosol scavenging and source regions, J. Geophys. Res. Atmos., 116(D8), n/a-n/a, doi:10.1029/2010JD015096, 2011.

Breider, T. J., Mickley, L. J., Jacob, D. J., Wang, Q., Fisher, J. A., Chang, R. Y.-W. and Alexander, B.: Annual distributions and sources of Arctic aerosol components, aerosol optical depth, and aerosol absorption, J. Geophys. Res. Atmos., 119(7), 4107–4124, doi:10.1002/2013JD020996, 2014.

Brock, C. A., Cozic, J., Bahreini, R., Froyd, K. D., Middlebrook, A. M., McComiskey, A., Brioude, J., Cooper, O. R., Stohl, A., Aikin, K. C., de Gouw, J. A., Fahey, D. W., Ferrare, R. A., Gao, R.-S., Gore, W., Holloway, J. S., Hübler, G., Jefferson, A., Lack, D. A., Lance, S., Moore, R. H., Murphy, D. M., Nenes, A., Novelli, P. C., Nowak, J. B., Ogren, J. A., Peischl, J., Pierce, R. B., Pilewskie, P., Quinn, P. K., Ryerson, T. B., Schmidt, K. S., Schwarz, J. P., Sodemann, H., Spackman, J. R., Stark, H., Thomson, D. S., Thornberry, T., Veres, P., Watts, L. A., Warneke, C. and Wollny, A. G.: Characteristics, sources, and transport of aerosols measured in spring 2008 during the aerosol, radiation, and cloud processes affecting Arctic Climate (ARCPAC) Project, Atmos. Chem. Phys., 11(6), 2423–2453, doi:10.5194/acp-11-2423-2011, 2011.

Chin, M., Diehl, T., Ginoux, P. and Malm, W.: Intercontinental transport of pollution and dust aerosols: implications for regional air quality, Atmos. Chem. Phys., 7(21), 5501–5517, doi:10.5194/acp-7-5501-2007, 2007.

Clarke, A. D. and Noone, K. J.: Soot in the Arctic snowpack: a cause for perturbations in radiative transfer, Atmos. Environ., 19(12), 2045–2053, doi:10.1016/0004-6981(85)90113-1, 1985.

Cohen, J. L., Furtado, J. C., Barlow, M. A., Alexeev, V. A. and Cherry, J. E.: Arctic warming, increasing snow cover and widespread boreal winter cooling, Environ. Res. Lett., 7(1), 14007, 2012.

D'Allura, A., Kulkarni, S., Carmichael, G. R., Finardi, S., Adhikary, B., Wei, C., Streets, D., Zhang, Q., Pierce, R. B., Al-Saadi, J. a., Diskin, G. and Wennberg, P.: Meteorological and air quality forecasting using the WRF–STEM model during the 2008 ARCTAS field campaign, Atmos. Environ., 45(38), 6901–6910, doi:10.1016/j.atmosenv.2011.02.073, 2011.

Delene, D. J. and Ogren, J. A.: Variability of Aerosol Optical Properties at Four North American Surface Monitoring Sites, J. Atmos. Sci., 59(6), 1135–1150, doi:10.1175/1520-0469(2002)059<1135:VOAOPA>2.0.CO;2, 2002.

Eckhardt, S., Quennehen, B., Berntsen, T. K., Cherian, R., Christensen, J. H., Collins, W., Crepinsek, S., Daskalakis, N., Flanner, M., Herber, A., Heyes, C., Huang, L., Kanakidou, M., Klimont, Z., Langner, J., Law, K. S., Lund, M. T., Mahmood, R., Massling, A., Myriokefalitakis, S., Nielsen, I. E., Quaas, J., Quinn, P. K., Rumbold, S. T., Schulz, M., Sharma, S., Skeie, R. B., Skov, H., Uttal, T. and Stohl, A.: Current model

capabilities for simulating black carbon and sulfate concentrations in the Arctic atmosphere : a multi-model evaluation, , (April), 9413–9433, doi:10.5194/acp-15-9413-2015, 2015.

Fisher, J. A., Jacob, D. J., Purdy, M. T., Kopacz, M., Le Sager, P., Carouge, C. C., Holmes, C. D., Yantosca, R. M., Batchelor, R. L. and Strong, K.: Source attribution and interannual variability of Arctic pollution in spring constrained by aircraft (ARCTAS, ARCPAC) and satellite (AIRS) observations of carbon monoxide, 2010.

Flanner, M. G., Zender, C. S., Randerson, J. T. and Rasch, P. J.: Present-day climate forcing and response from black carbon in snow, J. Geophys. Res., 112(D11), D11202, doi:10.1029/2006JD008003, 2007.

Fuelberg, H. E., Harrigan, D. L. and Sessions, W.: A meteorological overview of the ARCTAS 2008 mission, Atmos. Chem. Phys., 10(2), 817–842, doi:10.5194/acp-10-817-2010, 2010.

Hansen, J. and Nazarenko, L.: Soot climate forcing via snow and ice albedos, Proc. Natl Acad. Sci. USA, 101, 423–428 [online] Available from: http://dx.doi.org/10.1073/pnas.2237157100, 2004.

Hansen, J. E. and Sato, M.: Trends of measured climate forcing agents, Proc. Natl Acad. Sci. USA, 98, 14778–14783 [online] Available from: http://dx.doi.org/10.1073/pnas.261553698, 2001.

IPCC: Climate Change 2007: The Physical Science Basis [mdash] Contribution of Working Group I to the Fourth Assessment Report of the Intergovernmental Panel on Climate Change [Solomon, S., D. Qin, M. Manning, Z. Chen, M. Marquis, K.B. Averyt, M. Tignor and H.L., Cambridge University Press, Cambridge, UK and New York, US., 2007.

IPCC: Climate change 2013: the physical science basis: Working Group I contribution to the Fifth assessment report of the Intergovernmental Panel on Climate Change [Stocker, T.F., D. Qin, G.-K. Plattner, M. Tignor, S.K. Allen, J. Boschung, A. Nauels, Y. Xia, V., Cambridge University Press, Cambridge., 2013.

Jacob, D. J., Crawford, J. H., Maring, H., Clarke, a. D., Dibb, J. E., Emmons, L. K., Ferrare, R. a., Hostetler, C. a., Russell, P. B., Singh, H. B., Thompson, a. M., Shaw, G. E., McCauley, E., Pederson, J. R. and Fisher, J. a.: The Arctic Research of the Composition of the Troposphere from Aircraft and Satellites (ARCTAS) mission: design, execution, and first results, Atmos. Chem. Phys., 10(11), 5191–5212, doi:10.5194/acp-10-5191-2010, 2010.

Jacobson, M. Z.: Control of fossil-fuel particulate black carbon plus organic matter, possibly the most effective method of slowing global warming, J. Geophys. Res., 107 [online] Available from: http://dx.doi.org/10.1029/2001JD001376, 2002.

Janssens-Maenhout, G., Crippa, M., Guizzardi, D., Dentener, F., Muntean, M., Pouliot, G., Keating, T., Zhang, Q., Kurokawa, J., Wankmüller, R., van der Gon, H., Kuenen, J. J. P., Klimont, Z., Frost, G., Darras, S., Koffi,

B. and Li, M.: HTAP_v2.2: a mosaic of regional and global emission grid maps for 2008 and 2010 to study hemispheric transport of air pollution, Atmos. Chem. Phys., 15(19), 11411–11432, doi:10.5194/acp-15-11411-2015, 2015.

Koch, D. and Hansen, J.: Distant origins of Arctic black carbon: A Goddard Institute for Space Studies ModelE experiment, J. Geophys. Res., 110(D4), D04204, doi:10.1029/2004JD005296, 2005.

Koch, D., Bond, T. C., Streets, D., Unger, N. and van der Werf, G. R.: Global impacts of aerosols from particular source regions and sectors, J. Geophys. Res., 112(D2), D02205, doi:10.1029/2005JD007024, 2007.

Koch, D., Schulz, M., Kinne, S., McNaughton, C., Spackman, J. R., Balkanski, Y., Bauer, S., Berntsen, T., Bond, T. C., Boucher, O., Chin, M., Clarke, A., De Luca, N., Dentener, F., Diehl, T., Dubovik, O., Easter, R., Fahey, D. W., Feichter, J., Fillmore, D., Freitag, S., Ghan, S., Ginoux, P., Gong, S., Horowitz, L., Iversen, T., Kirkevåg, A., Klimont, Z., Kondo, Y., Krol, M., Liu, X., Miller, R., Montanaro, V., Moteki, N., Myhre, G., Penner, J. E., Perlwitz, J., Pitari, G., Reddy, S., Sahu, L., Sakamoto, H., Schuster, G., Schwarz, J. P., Seland, Ø., Stier, P., Takegawa, N., Takemura, T., Textor, C., van Aardenne, J. A. and Zhao, Y.: Evaluation of black carbon estimations in global aerosol models, Atmos. Chem. Phys., 9(22), 9001–9026, doi:10.5194/acp-9-9001-2009, 2009.

Kondo, Y., Matsui, H., Moteki, N., Sahu, L., Takegawa, N., Kajino, M., Zhao, Y., Cubison, M. J., Jimenez, J. L., Vay, S., Diskin, G. S., Anderson, B., Wisthaler, A., Mikoviny, T., Fuelberg, H. E., Blake, D. R., Huey, G., Weinheimer, A. J., Knapp, D. J. and Brune, W. H.: Emissions of black carbon, organic, and inorganic aerosols from biomass burning in North America and Asia in 2008, J. Geophys. Res. Atmos., 116(D8), n/a--n/a, doi:10.1029/2010JD015152, 2011.

Kulkarni, S., Sobhani, N., Shafer, M. M., Schauer, J. J., Solomon, P. A., Saide, P. E., Spak, S. N., Cheng, Y. F., Gon, H. A. C. D. Van Der, Lu, Z., Streets, D. G., Miller-Schulze, J. P., Shafer, M. M., Schauer, J. J., Solomon, P. A., Saide, P. E., Spak, S. N. Cheng, Y. F., Denier van der Gon, H. A. C., Lu, Z., Streets, D. G., Janssens-Maenhout, G., Wiedinmyer, C., Lantz, J., Artamonova, M., Chen, B., Imashev, S., Sverdlik, L., Deminter, J. T., Adhikary, B., D'Allura, A., Wei, C. and Carmichael, G. R.: Source sector and region contributions to BC and PM 2.5 in Central Asia, Atmos. Chem. Phys., 15(1), 1–18, doi:10.5194/acp-15-1-2015, 2015.

Law, K. S. and Stohl, A.: Arctic air pollution: origins and impacts., Science, 315(5818), 1537–40, doi:10.1126/science.1137695, 2007.

Law, K. S., Stohl, A., Quinn, P. K., Brock, C. A., Burkhart, J. F., Paris, J.-D., Ancellet, G., Singh, H. B., Roiger, A., Schlager, H., Dibb, J., Jacob, D. J., Arnold, S. R., Pelon, J. and Thomas, J. L.: Arctic Air Pollution: New

Insights from POLARCAT-IPY, Bull. Am. Meteorol. Soc., 95(12), 1873–1895, doi:10.1175/BAMS-D-13-00017.1, 2014.

Law, K. S., Roiger, A., Thomas, J. L., Marelle, L., Raut, J.-C., Dalsøren, S., Fuglestvedt, J., Tuccella, P., Weinzierl, B. and Schlager, H.: Local Arctic air pollution: Sources and impacts, Ambio, 46(3), 453–463, doi:10.1007/s13280-017-0962-2, 2017.

Liousse, C., Penner, J. E., Chuang, C., Walton, J. J., Eddleman, H. and Cachier, H.: A global three-dimensional model study of carbonaceous aerosols, J. Geophys. Res. Atmos., 101(D14), 19411–19432, doi:10.1029/95JD03426, 1996.

Liu, D., Quennehen, B., Darbyshire, E., Allan, J. D., Williams, P. I., Taylor, J. W., Bauguitte, S. J.-B., Flynn, M. J., Lowe, D., Gallagher, M. W., Bower, K. N., Choularton, T. W. and Coe, H.: The importance of Asia as a source of black carbon to the European Arctic during springtime 2013, Atmos. Chem. Phys., 15(20), 11537–11555, doi:10.5194/acp-15-11537-2015, 2015.

Liu, J., Fan, S., Horowitz, L. W. and Levy, H.: Evaluation of factors controlling long-range transport of black carbon to the Arctic, J. Geophys. Res., 116(D4), D04307, doi:10.1029/2010JD015145, 2011.

Marelle, L., Thomas, J. L., Raut, J.-C., Law, K. S., Jalkanen, J.-P., Johansson, L., Roiger, A., Schlager, H., Kim, J. and Reiter, A.: Air quality and radiative impacts of Arctic shipping emissions in the summertime in northern Norway: from the local to the regional scale, Atmos. Chem. Phys., 16(4), 2359–2379, 2016.

Matsui, H., Kondo, Y., Moteki, N., Takegawa, N., Sahu, L. K., Zhao, Y., Fuelberg, H. E., Sessions, W. R., Diskin, G., Blake, D. R., Wisthaler, a. and Koike, M.: Seasonal variation of the transport of black carbon aerosol from the Asian continent to the Arctic during the ARCTAS aircraft campaign, J. Geophys. Res., 116(D5), D05202, doi:10.1029/2010JD015067, 2011.

McConnell, J. R.: 20th-century industrial black carbon emissions altered arctic climate forcing, Science (80-.)., 317, 1381–1384 [online] Available from: http://dx.doi.org/10.1126/science.1144856, 2007.

McNaughton, C. S., Clarke, a. D., Freitag, S., Kapustin, V. N., Kondo, Y., Moteki, N., Sahu, L., Takegawa, N., Schwarz, J. P., Spackman, J. R., Watts, L., Diskin, G., Podolske, J., Holloway, J. S., Wisthaler, a., Mikoviny, T., de Gouw, J., Warneke, C., Jimenez, J., Cubison, M., Howell, S. G., Middlebrook, a., Bahreini, R., Anderson, B. E., Winstead, E., Thornhill, K. L., Lack, D., Cozic, J. and Brock, C. a.: Absorbing aerosol in the troposphere of the Western Arctic during the 2008 ARCTAS/ARCPAC airborne field campaigns, Atmos. Chem. Phys., 11(15), 7561–7582, doi:10.5194/acp-11-7561-2011, 2011.

Qi, L., Li, Q., Li, Y. and He, C.: Factors controlling black carbon distribution in the Arctic, Atmos. Chem. Phys., 17(2), 1037–1059, doi:10.5194/acp-17-1037-2017, 2017a.

Qi, L., Li, Q., Henze, D. K., Tseng, H.-L. and He, C.: Sources of Springtime Surface Black Carbon in the Arctic: An Adjoint Analysis, Atmos. Chem. Phys. Discuss., 2017, 1–32, doi:10.5194/acp-2016-1112, 2017b.

Quinn, P. K., Miller, T. L., Bates, T. S. and Shaw, G. E.: A 3-year record of simultaneously measured aerosol chemical and optical properties at Barrow , Alaska, , 107, 2002.

5   Quinn, P. K., Shaw, G., ANDREWS, E., DUTTON, E. G., RUOHO-AIROLA, T. and GONG, S. L.: Arctic haze: current trends and knowledge gaps, Tellus B, 59(1), 99–114, doi:10.1111/j.1600-0889.2006.00238.x, 2007.

Quinn, P. K., Bates, T. S., Baum, E., Doubleday, N., Fiore, A. M., Flanner, M., Fridlind, A., Garrett, T. J., Koch, D., Menon, S., Shindell, D., Stohl, A. and Warren, S. G.: Short-lived pollutants in the Arctic: their climate impact and possible mitigation strategies, Atmos. Chem. Phys., 8(6), 1723–1735, doi:10.5194/acp-8-1723-
10   2008, 2008.

Raatz, W. E. and Shaw, G. E.: Long-range tropospheric transport of pollution aerosols into the Alaskan Arctic, J. Clim. Appl. Meteorol., 23(7), 1052–1064, 1984.

Ramanathan, V. and Carmichael, G.: Global and regional climate changes due to black carbon, Nat. Geosci., 1(4), 221–227, doi:10.1038/ngeo156, 2008.

15   Rosen, H., Novakov, T. and Bodhaine, B. A.: Soot in the Arctic, Atmos. Environ., 15(8), 1371–1374, doi:https://doi.org/10.1016/0004-6981(81)90343-7, 1981.

Schmale, J., Schneider, J., Ancellet, G., Quennehen, B., Stohl, A., Sodemann, H., Burkhart, J. F., Hamburger, T., Arnold, S. R., Schwarzenboeck, A., Borrmann, S. and Law, K. S.: Source identification and airborne chemical characterisation of aerosol pollution from long-range transport over Greenland during POLARCAT
20   summer campaign 2008, Atmos. Chem. Phys., 11(19), 10097–10123, doi:10.5194/acp-11-10097-2011, 2011.

Schnell, R. C.: Arctic haze and the Arctic Gas and Aerosol Sampling Program (AGASP), Geophys. Res. Lett., 11(5), 361–364, doi:10.1029/GL011i005p00361, 1984.

Screen, J. A. and Simmonds, I.: The central role of diminishing sea ice in recent Arctic temperature amplification, Nature, 464(7293), 1334–1337 [online] Available from:
25   http://dx.doi.org/10.1038/nature09051, 2010.

Sharma, S., Brook, J. R., Cachier, H., Chow, J., Gaudenzi, A. and Lu, G.: Light absorption and thermal measurements of black carbon in different regions of Canada, J. Geophys. Res. Atmos., 107(D24), AAC 11-1--AAC 11-11, doi:10.1029/2002JD002496, 2002.

Sharma, S., Lavoué, D., Cachier, H., Barrie, L. A. and Gong, S. L.: Long-term trends of the black carbon
30   concentrations in the Canadian Arctic, J. Geophys. Res. Atmos., 109(D15), n/a--n/a, doi:10.1029/2003JD004331, 2004.

Sharma, S., Ishizawa, M., Chan, D., Lavoué, D., Andrews, E., Eleftheriadis, K. and Maksyutov, S.: 16-year simulation of Arctic black carbon: Transport, source contribution, and sensitivity analysis on deposition, J. Geophys. Res. Atmos., 118(2), 943–964, doi:10.1029/2012JD017774, 2013a.

Sharma, S., Ogren, J. A., Jefferson, A., Eleftheriadis, K., Chan, E., Quinn, P. K. and Burkhart, J. F.: Equivalent Black Carbon in the Arctic, , (Figure 1), 2013b.

Sharma, S., Leaitch, W. R., Huang, L., Veber, D., Kolonjari, F., Zhang, W., Hanna, S. J., Bertram, A. K. and Ogren, J. A.: An Evaluation of three methods for measuring black carbon at Alert, Canada, Atmos. Chem. Phys. Discuss., 2017, 1–42, doi:10.5194/acp-2017-339, 2017.

Shaw, G. E.: The Arctic haze phenomenon, Bull. Am. Meteorol. Soc., 76(12), 2403–2413, 1995.

Shindell, D. T., Chin, M., Dentener, F., Doherty, R. M., Faluvegi, G., Fiore, a. M., Hess, P., Koch, D. M., MacKenzie, I. a., Sanderson, M. G., Schultz, M. G., Schulz, M., Stevenson, D. S., Teich, H., Textor, C., Wild, O., Bergmann, D. J., Bey, I., Bian, H., Cuvelier, C., Duncan, B. N., Folberth, G., Horowitz, L. W., Jonson, J., Kaminski, J. W., Marmer, E., Park, R., Pringle, K. J., Schroeder, S., Szopa, S., Takemura, T., Zeng, G., Keating, T. J. and Zuber, a.: A multi-model assessment of pollution transport to the Arctic, Atmos. Chem. Phys., 8(17), 5353–5372, doi:10.5194/acp-8-5353-2008, 2008.

Sinha, P. R., Kondo, Y., Koike, M., Ogren, J. A., Jefferson, A., Barrett, T. E., Sheesley, R. J., Ohata, S., Moteki, N., Coe, H., Liu, D., Irwin, M., Tunved, P., Quinn, P. K. and Zhao, Y.: Evaluation of ground-based black carbon measurements by filter-based photometers at two Arctic sites, J. Geophys. Res. Atmos., 122(6), 3544–3572, doi:10.1002/2016JD025843, 2017.

Sobhani, N.: Applications, Performance Analysis, and Optimization of Weather and Air Quality Models, University of Iowa., 2017.

Spackman, J. R., Gao, R. S., Neff, W. D., Schwarz, J. P., Watts, L. A., Fahey, D. W., Holloway, J. S., Ryerson, T. B., Peischl, J. and Brock, C. A.: Aircraft observations of enhancement and depletion of black carbon mass in the springtime Arctic, Atmos. Chem. Phys., 10(19), 9667–9680, doi:10.5194/acp-10-9667-2010, 2010.

Stohl, A.: Characteristics of atmospheric transport into the Arctic troposphere, J. Geophys. Res., 111(D11), D11306, doi:10.1029/2005JD006888, 2006.

Stohl, A., Klimont, Z., Eckhardt, S., Kupiainen, K., Shevchenko, V. P., Kopeikin, V. M. and Novigatsky, A. N.: Black carbon in the Arctic: the underestimated role of gas flaring and residential combustion emissions, Atmos. Chem. Phys., 13(17), 8833–8855, doi:10.5194/acp-13-8833-2013, 2013.

Stohl, a., Andrews, E., Burkhart, J. F., Forster, C., Herber, a., Hoch, S. W., Kowal, D., Lunder, C., Mefford, T., Ogren, J. a., Sharma, S., Spichtinger, N., Stebel, K., Stone, R., Ström, J., Tørseth, K., Wehrli, C. and Yttri, K.

E.: Pan-Arctic enhancements of light absorbing aerosol concentrations due to North American boreal forest fires during summer 2004, J. Geophys. Res. Atmos., 111, 1–20, doi:10.1029/2006JD007216, 2006.

Streets, D. G., Yan, F., Chin, M., Diehl, T., Mahowald, N., Schultz, M., Wild, M., Wu, Y. and Yu, C.: Anthropogenic and natural contributions to regional trends in aerosol optical depth, 1980–2006, J. Geophys. Res. Atmos., 114(D10), n/a--n/a, doi:10.1029/2008JD011624, 2009.

Uno, I., Satake, S., Carmichael, G. R., Tang, Y., Wang, Z., Takemura, T., Sugimoto, N., Shimizu, A., Murayama, T., Cahill, T. A., Cliff, S., Uematsu, M., Ohta, S., Quinn, P. K. and Bates, T. S.: Numerical study of Asian dust transport during the springtime of 2001 simulated with the Chemical Weather Forecasting System (CFORS) model, J. Geophys. Res., 109(D19), n/a-n/a, doi:10.1029/2003jd004222, 2004.

Wang, Q., Jacob, D. J., Fisher, J. a., Mao, J., Leibensperger, E. M., Carouge, C. C., Le Sager, P., Kondo, Y., Jimenez, J. L., Cubison, M. J. and Doherty, S. J.: Sources of carbonaceous aerosols and deposited black carbon in the Arctic in winter-spring: implications for radiative forcing, Atmos. Chem. Phys., 11(23), 12453–12473, doi:10.5194/acp-11-12453-2011, 2011.

Warneke, C., Bahreini, R., Brioude, J., Brock, C. A., de Gouw, J. A., Fahey, D. W., Froyd, K. D., Holloway, J. S., Middlebrook, A., Miller, L., Montzka, S., Murphy, D. M., Peischl, J., Ryerson, T. B., Schwarz, J. P., Spackman, J. R. and Veres, P.: Biomass burning in Siberia and Kazakhstan as an important source for haze over the Alaskan Arctic in April 2008, Geophys. Res. Lett., 36(2), n/a--n/a, doi:10.1029/2008GL036194, 2009.

Warneke, C., Froyd, K. D., Brioude, J., Bahreini, R., Brock, C. A., Cozic, J., De Gouw, J. A., Fahey, D. W., Ferrare, R. and Holloway, J. S.: An important contribution to springtime Arctic aerosol from biomass burning in Russia, Geophys. Res. Lett., 37(1), 2010.

Weingartner, E., Saathoff, H., Schnaiter, M., Streit, N., Bitnar, B. and Baltensperger, U.: Absorption of light by soot particles: determination of the absorption coefficient by means of aethalometers, J. Aerosol Sci., 34(10), 1445–1463, doi:https://doi.org/10.1016/S0021-8502(03)00359-8, 2003.

Wiedinmyer, C., Akagi, S. K., Yokelson, R. J., Emmons, L. K., Al-Saadi, J. A., Orlando, J. J. and Soja, A. J.: The Fire INventory from NCAR (FINN): a high resolution global model to estimate the emissions from open burning, Geosci. Model Dev., 4(3), 625–641, doi:10.5194/gmd-4-625-2011, 2011.

Wiedinmyer, C., Yokelson, R. J. and Gullett, B. K.: Global Emissions of Trace Gases, Particulate Matter, and Hazardous Air Pollutants from Open Burning of Domestic Waste, Environ. Sci. Technol., 48(16), 9523–9530, doi:10.1021/es502250z, 2014.

Wiscombe, W. J. and Warren, S. G.: A Model for the Spectral Albedo of Snow. I: Pure Snow, J. Atmos. Sci.,

37(12), 2712–2733, doi:10.1175/1520-0469(1980)037<2712:AMFTSA>2.0.CO;2, 1980.

Xu, J., Martin, R. V, Morrow, A., Sharma, S., Huang, L., Leaitch, W. R., Burkart, J., Schulz, H., Zanatta, M., Willis, M. D., Henze, D. K., Lee, C. J., Herber, A. B. and Abbatt, J. P. D.: Source attribution of Arctic black carbon constrained by aircraft and surface measurements, Atmos. Chem. Phys. Discuss., 2017, 1–45, doi:10.5194/acp-2017-236, 2017.

7. Tables and Figures

Table 1: NASA ARCTAS Flight Categories for Spring and Summer 2008

Flight Season	Flight Categories	Flight Date	Flight Number
Spring Flights	Spring Alaska Local Flights	04/12/2008	08
		04/16/2008	09
	Spring Greenland Flights	04/04/2008	04
		04/05/2008	05
		04/08/2008	06
		04/09/2008	07
		04/17/2008	10
	Spring Transit Flights	04/01/2008	03
		04/19/2008	11
Summer Flights	Summer California Flights	06/18/2008	12
		06/20/2008	13
		06/22/2008	14
		06/24/2008	15
	Summer Canada Flights	06/29/2008	17
		07/01/2008	18
		07/04/2008	19
		07/05/2008	20
	Summer Canada Greenland Flights	07/08/2008	21
		07/09/2008	22
		07/10/2008	23
	Summer Transit Flights	06/26/2008	16
		07/13/2008	24

Table 2- Statistical summary of comparison of observed and modeled meteorological parameters for NASA ARCTAS spring and summer flights. Obs and Mdl denote observation and model data.

	Temperature (K)		Pressure (hpa)		Relative Humidity (%)		Wind Speed (m/s)	
	Obs	Mdl	Obs	Mdl	Obs	Mdl	Obs	Mdl
Mean	248.4	263.1	610.2	594.6	45.5	45.5	13.0	13.5
Standard Error	0.3	0.3	3.7	3.4	0.4	0.4	0.2	0.1
Median	245.4	265.7	554.9	569.0	43.4	43.4	9.7	11.5
Mode	225.0	231.4	1007.0	329.3	19.8	19.8	25.7	25.7
Standard Deviation	23.6	23.1	253.2	232.8	27.0	27.0	10.9	9.1
Range	94.8	93.6	818.9	817.2	117.1	117.1	56.2	43.4
Minimum	212.7	212.2	206.7	187.1	0.7	0.7	0.2	0.1
Maximum	307.4	305.8	1025.6	1004.2	117.8	117.8	56.4	43.5
R-Square	0.984		0.757		0.585		0.405	
Standard Error	32.463		314.263		34.059		12.553	
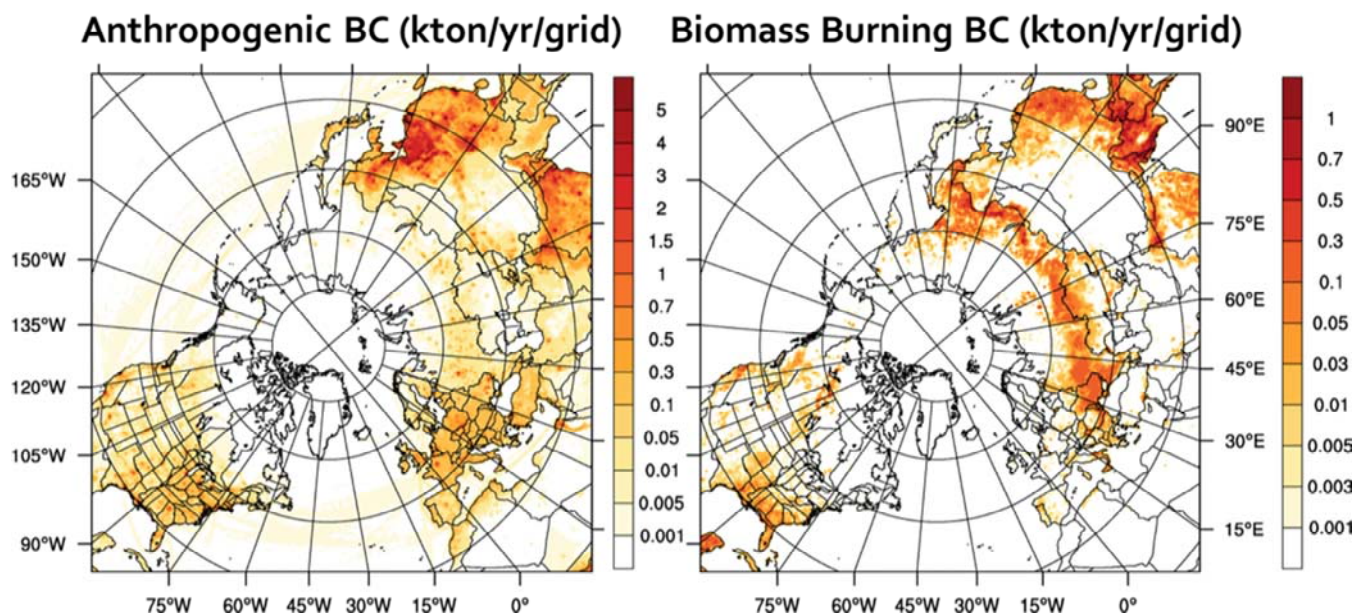
Figure 1: Spatial distribution of a) anthropogenic BC emissions and b) wildfire BC emissions in Gg/yr/grid.
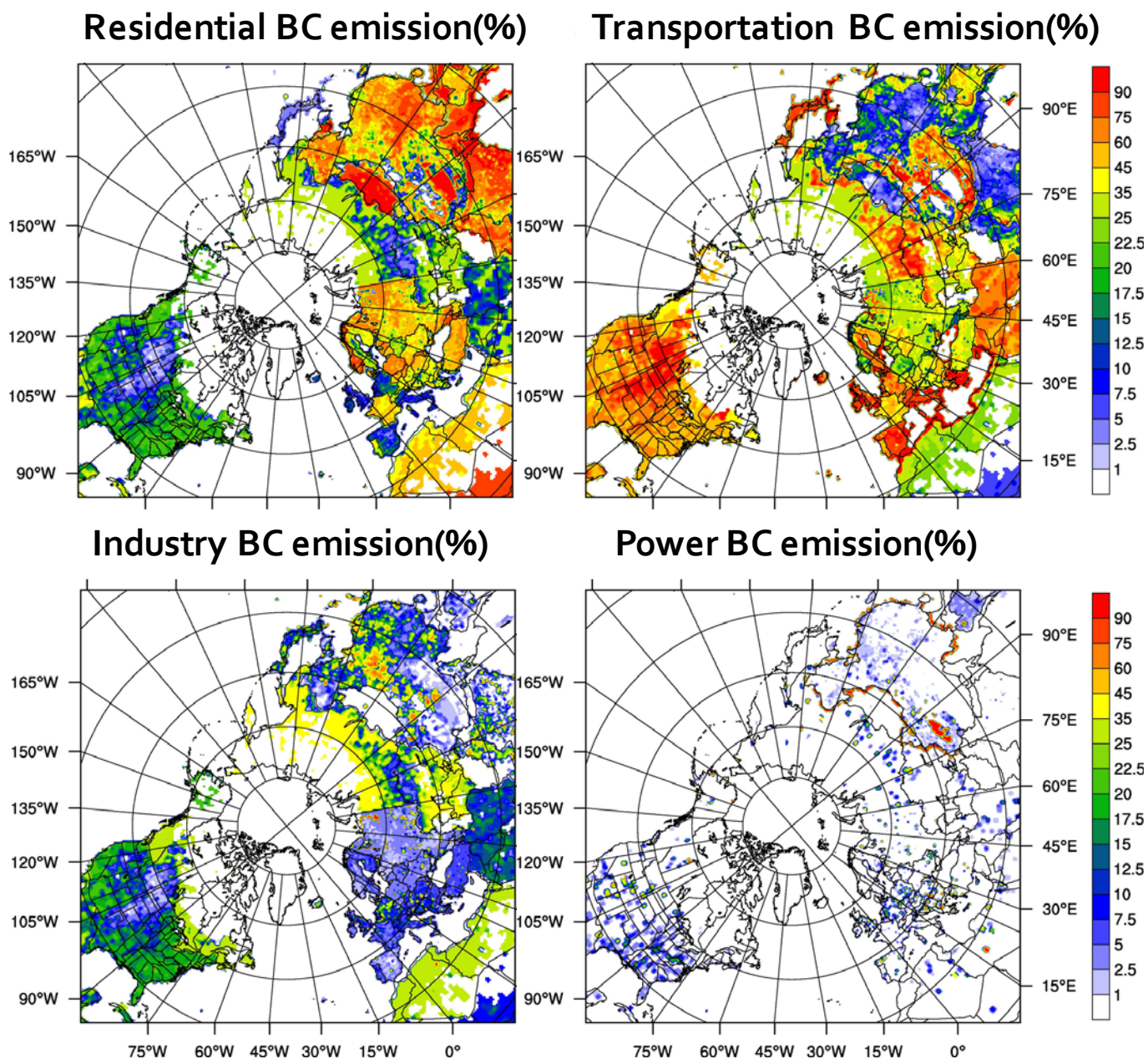
Figure 2: Spatial distribution of economic sectors (%) in total BC anthropogenic emissions.
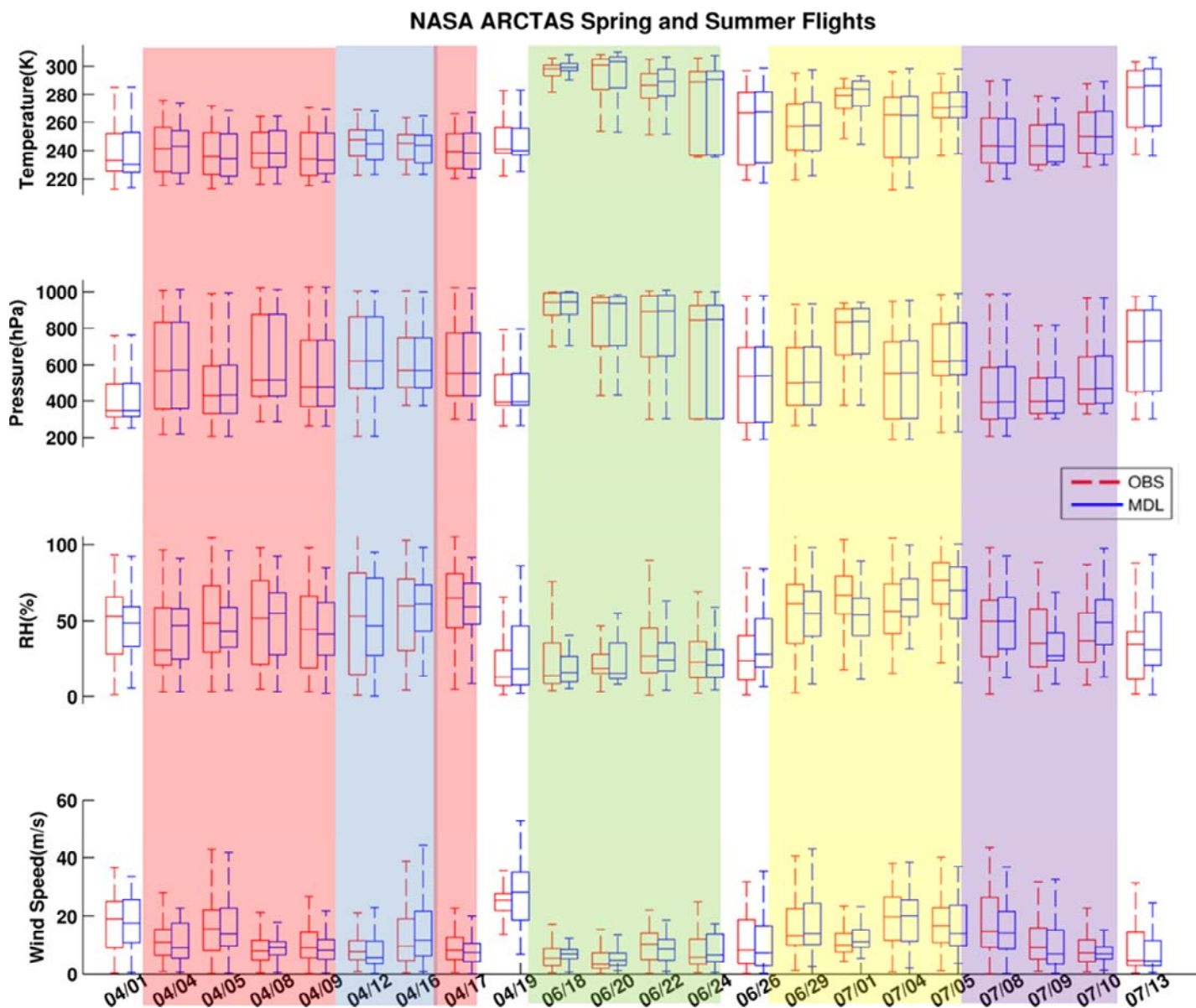
Figure 3: Comparison of key meteorological variables for NASA ARCTAS spring and summer flights. Each flight category is shaded with a different color and the spring and summer transition flights are not shaded. Spring Alaska local flights and spring Greenland flights are shaded blue and red respectively. Green, yellow, and purple shades denote the summer California flights, summer Canada flights, and summer Canada Greenland flights.
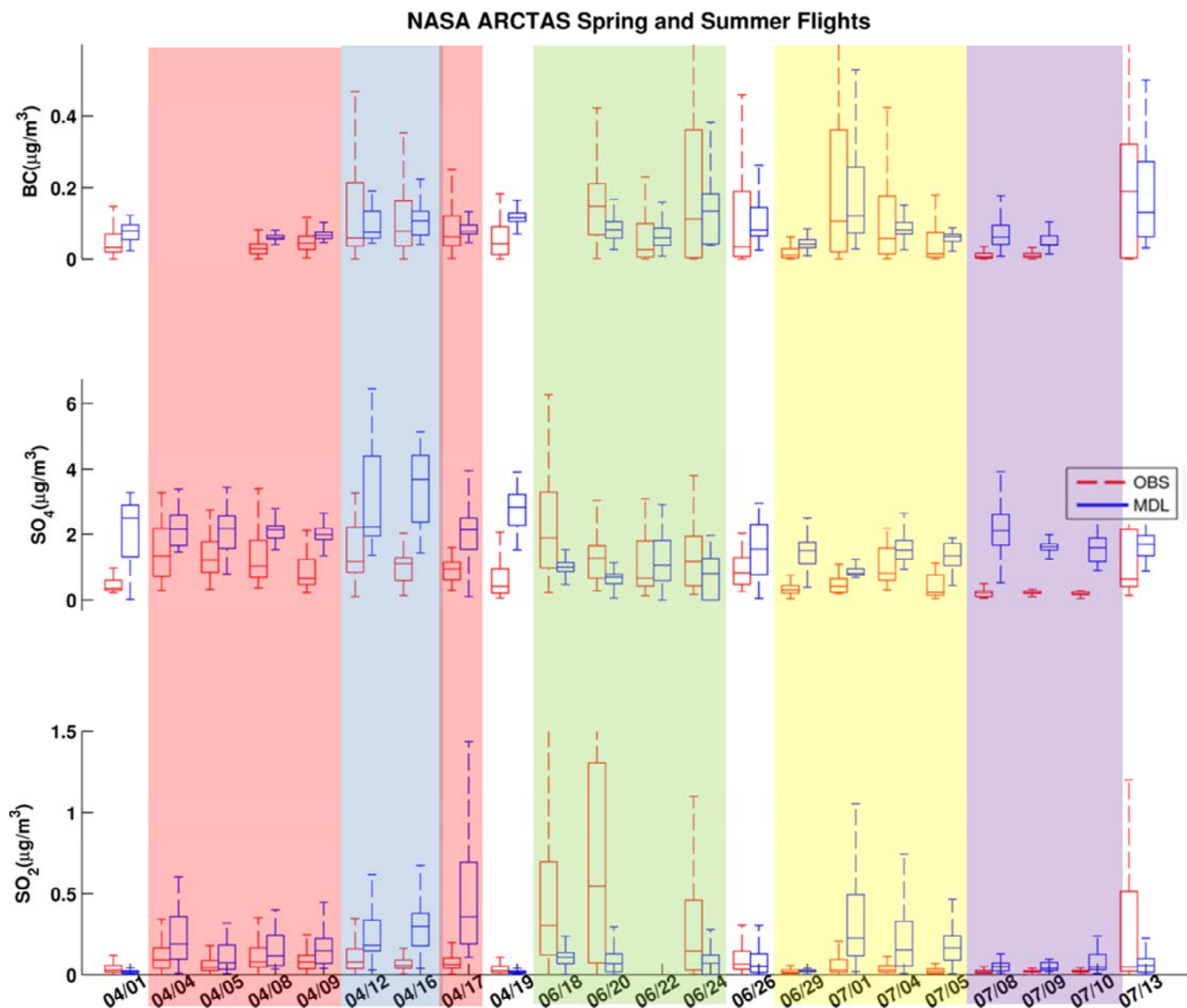
Figure 4: Comparison of BC, SO₄, and SO₂ for NASA ARCTAS spring and summer flights. Flight categories are shaded same as figure 3.
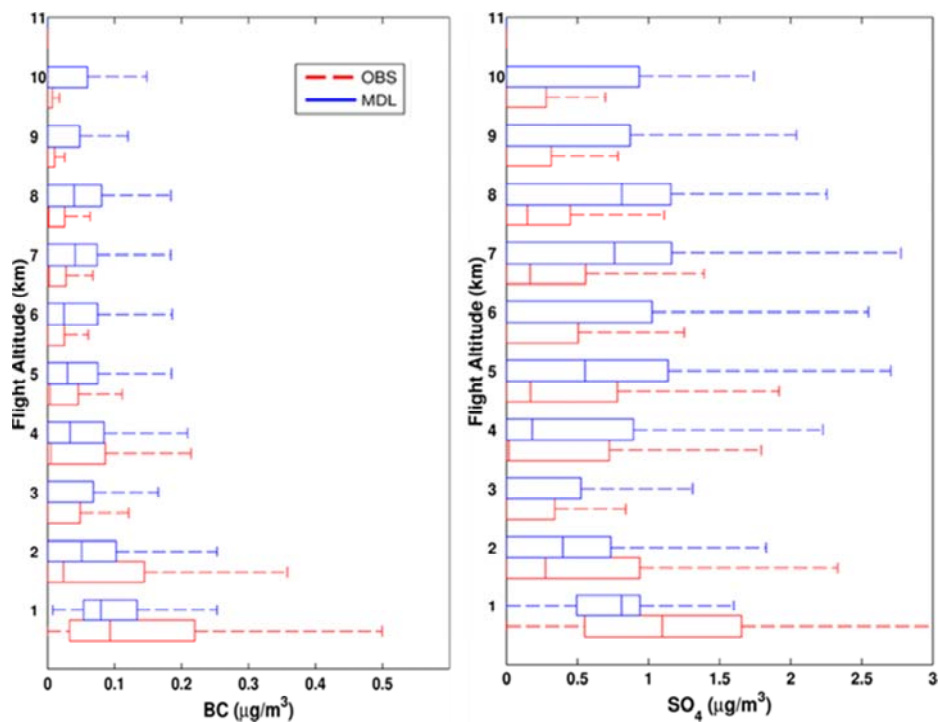
Figure 5: Comparison of Model and Observation BC and SO$_4$ for all ARCTAS flights.
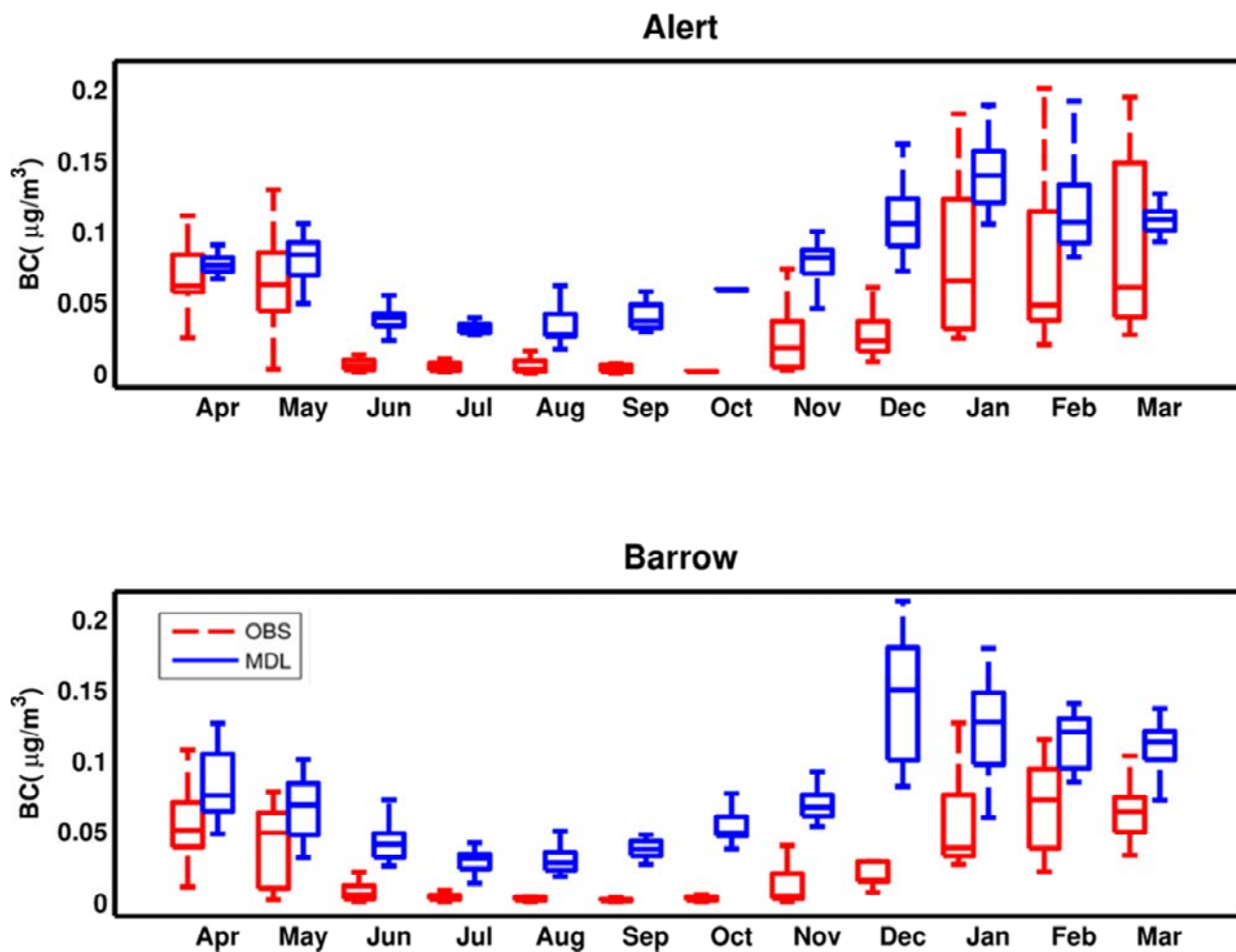
Figure 6: Comparison of simulated BC with observations shown as box-and-whisker plots over the simulations period at Alert (top panel) and Barrow (bottom panel) sites.
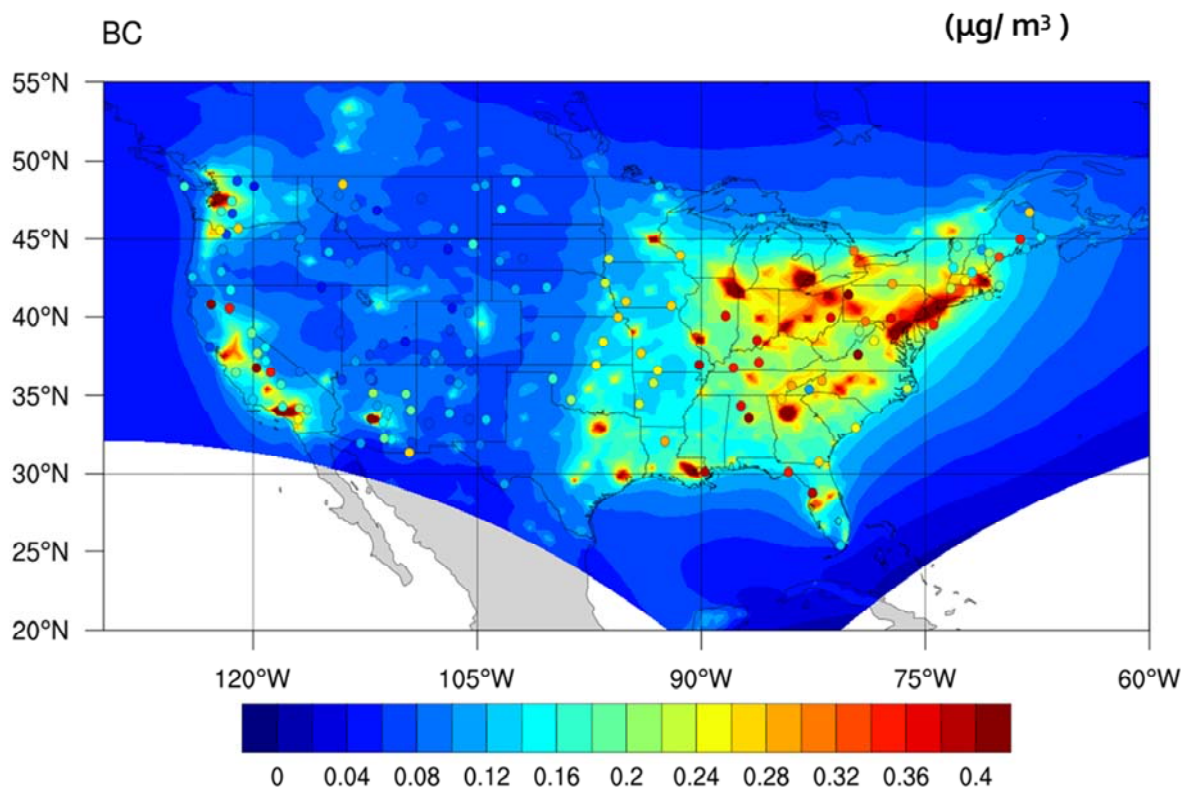
Figure 7: Annual average surface BC concentration over the U.S. The circles indicate IMPROVE sites with the color representing the BC concentration in μg/m³.
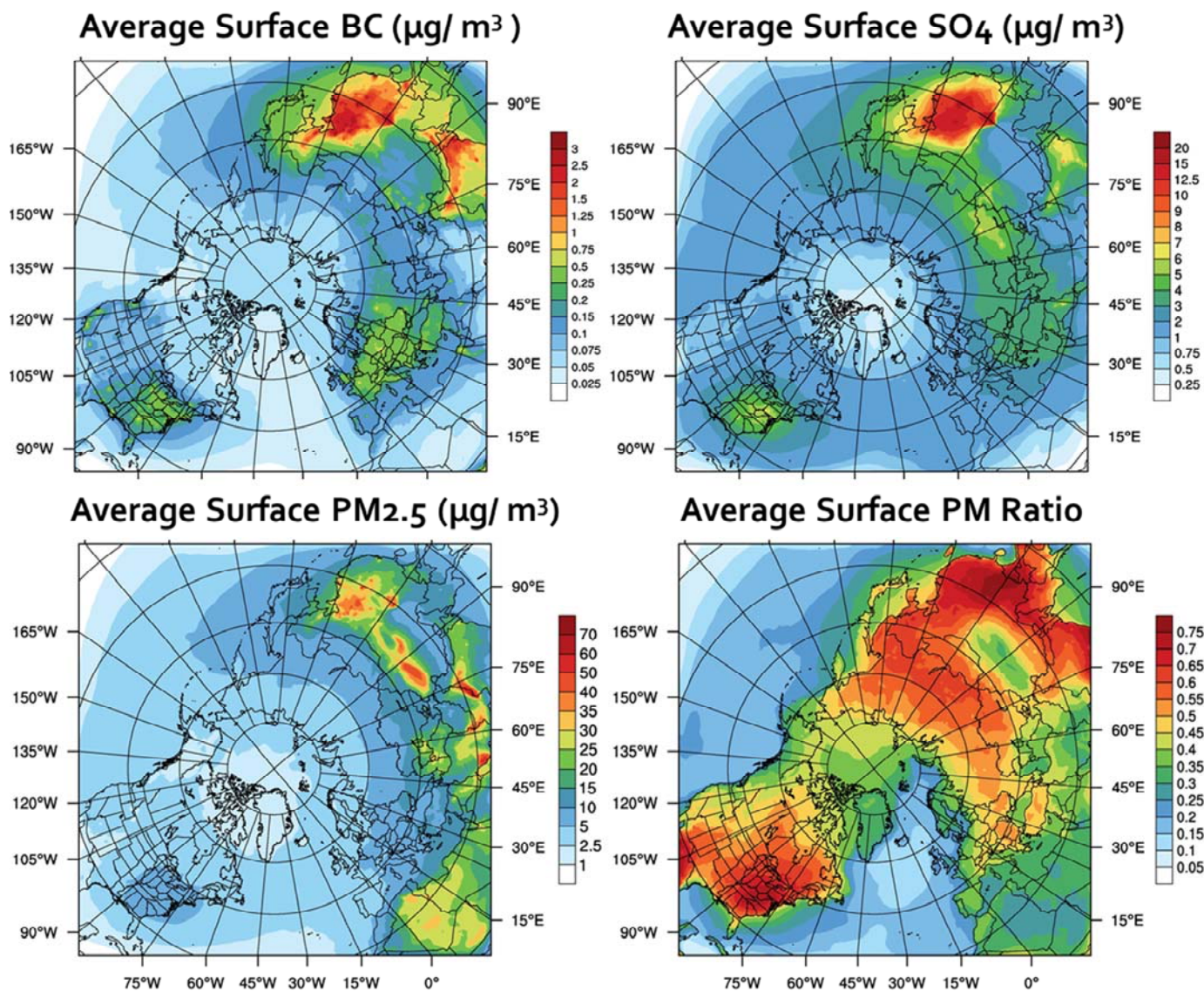
Figure 8: Spatial distributions of simulated BC (µg/m3), Dust (µg/m³), PM2.5 (µg/m³), and PM2.5/PM10 ratio averaged over the simulation period. The values on the map denote contour values at sharp gradients.
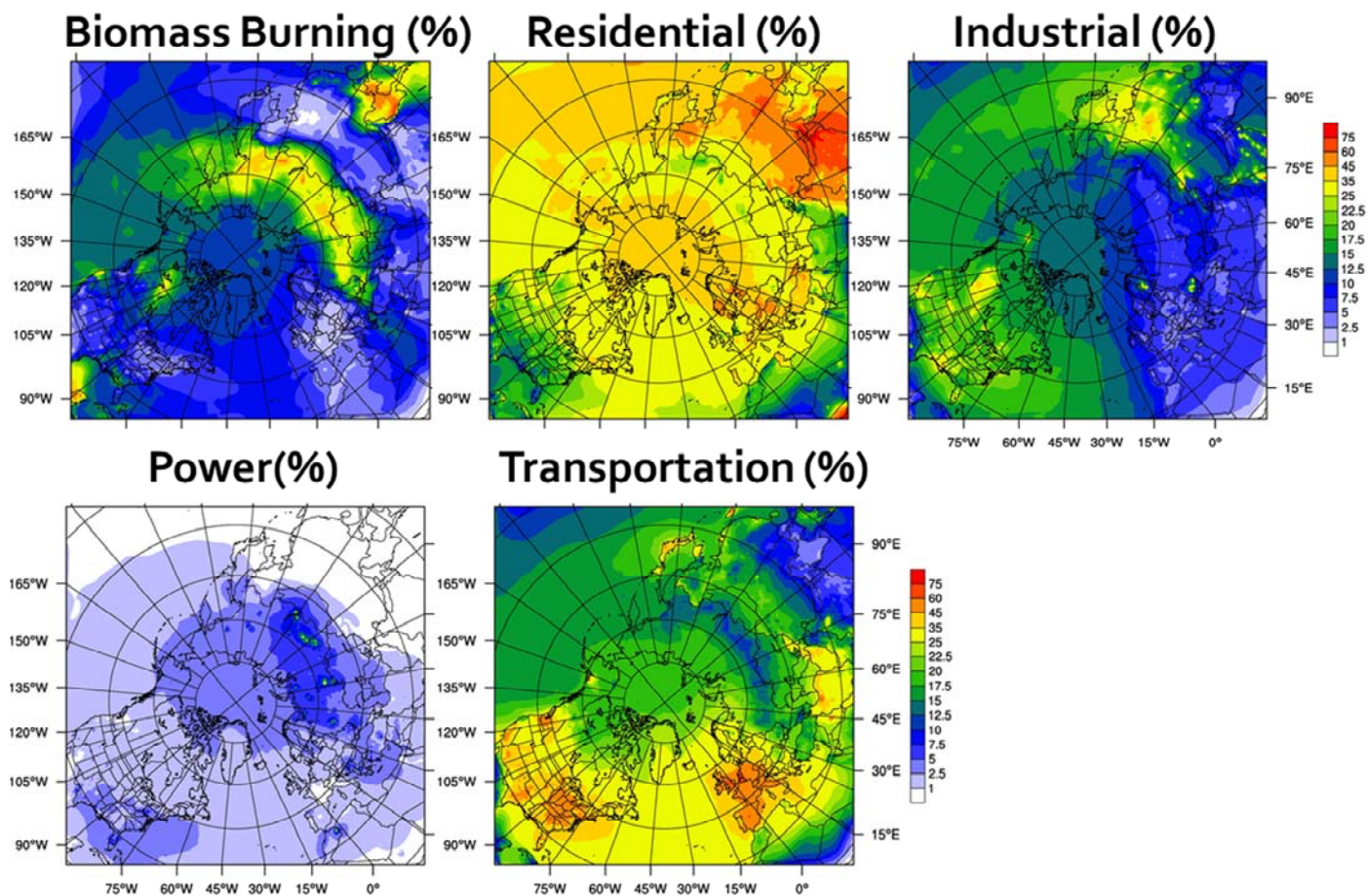
Figure 9: Spatial distribution of source sector contributions (%) to annual BC surface concentration over the entire domain.

Arctic Surface Concentration(μg/ m³)
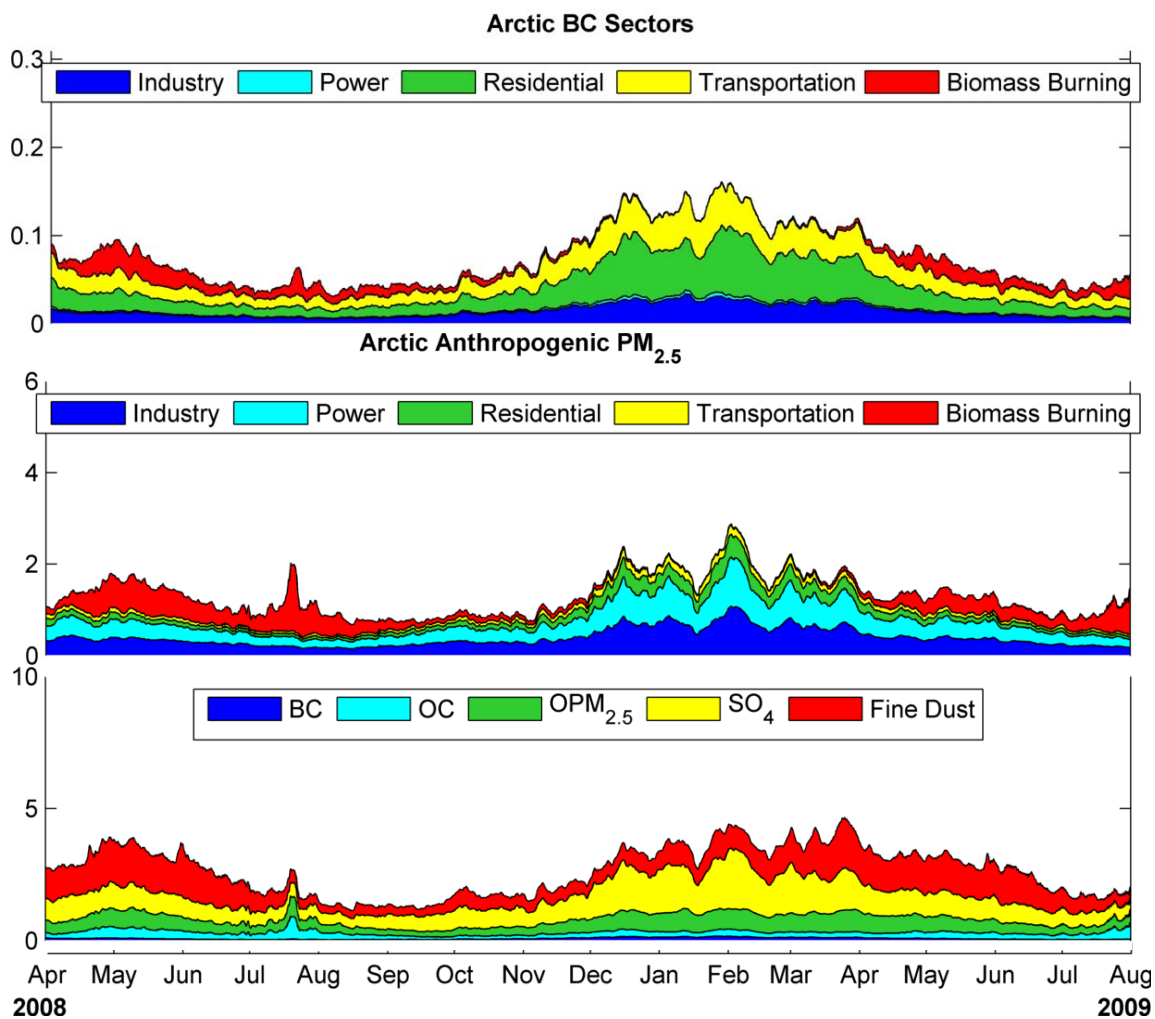
Figure 10: Time-series concentration and contribution of different sector to BC concentration (top panel) different sectors to PM$_{2.5}$ concentration (middle panel), and different PM$_{2.5}$ species (bottom panel).
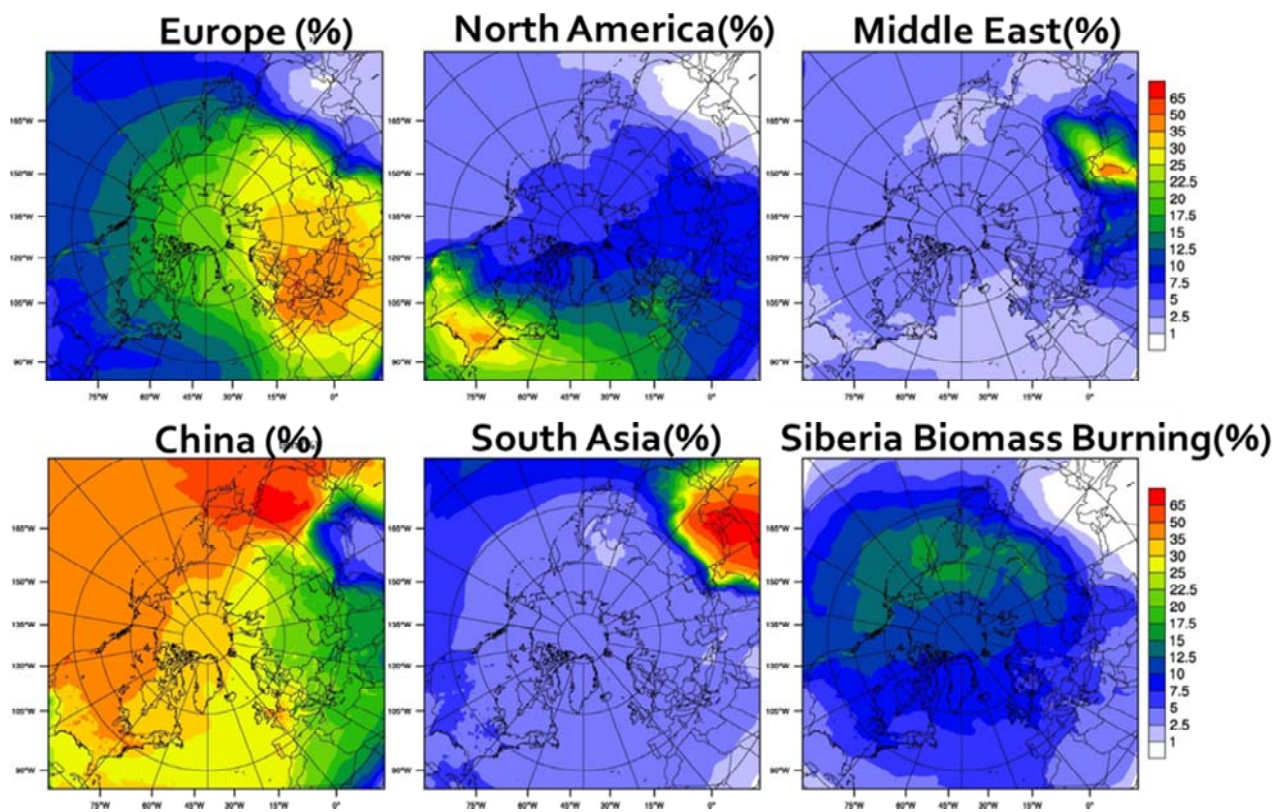
Figure 11: Spatial distribution of source region contributions (%) to annual BC surface concentration over the entire domain.
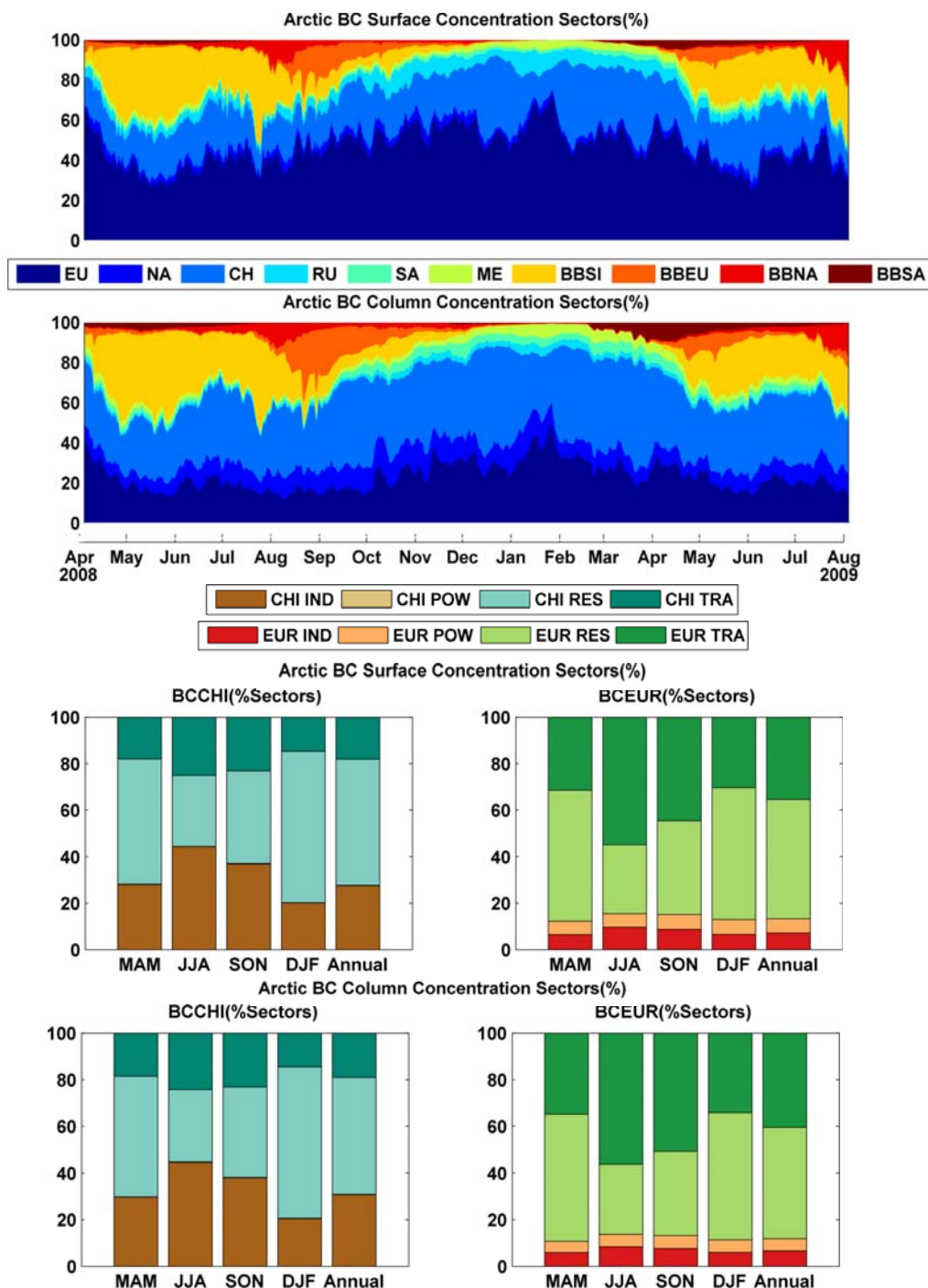
Figure 12: Seasonality of BC major geographical contributors to the Arctic average surface and column concentrations. The bar plots indicate the seasonality of contributions of various economic sectors from Europe or China to surface or column BC concentration.
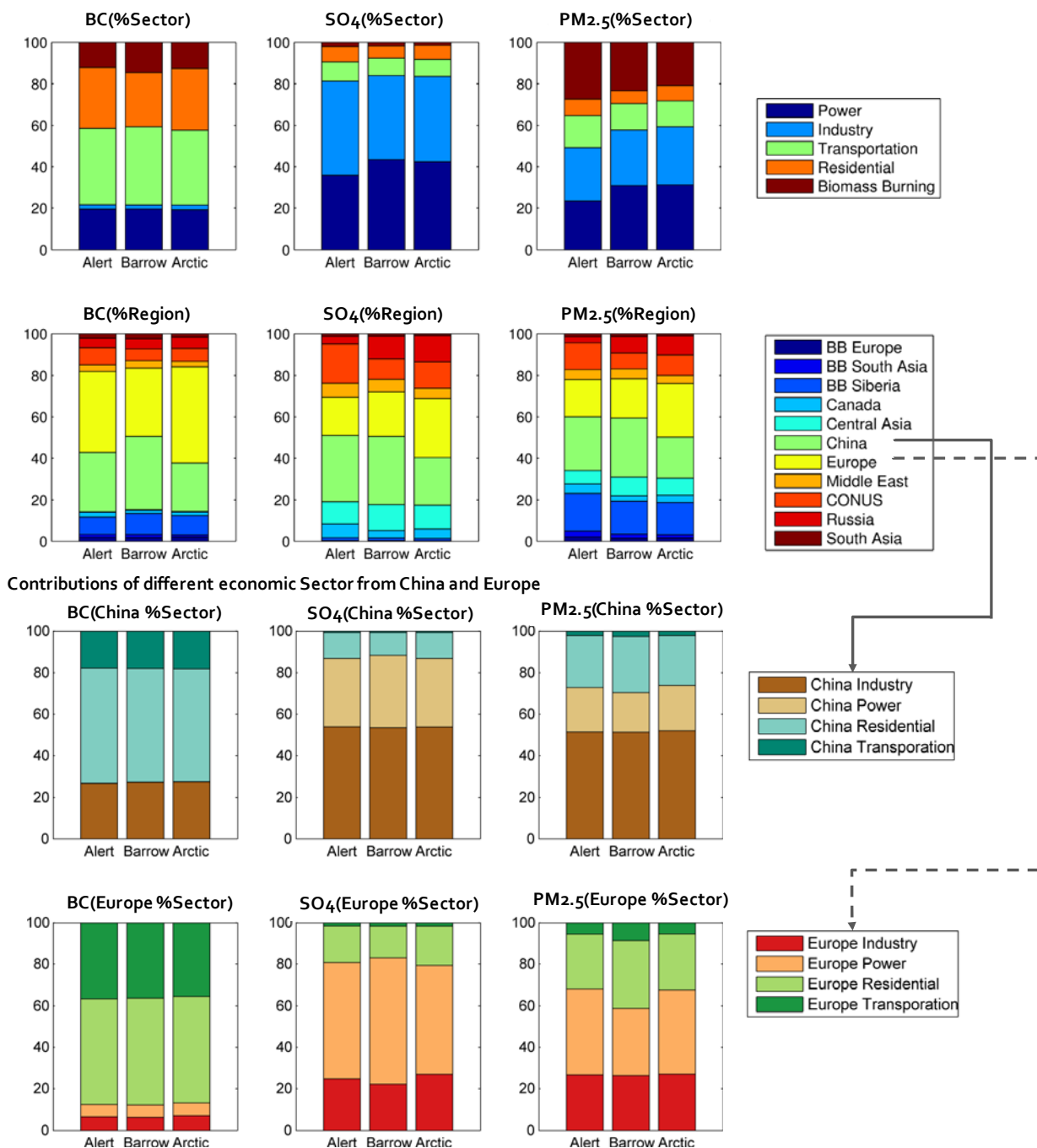
Figure 13: Summary of annual mean contributions to BC, SO₄, and PM₂.₅ by source sectors (top row), and source regions (2nd row) at Alert, Barrow, and over the Arctic regions. The bottom two rows of bar plots show the relative contributions of various economic sectors from either China (3rd row) or Europe (bottom row) to total China or Europe contributions to Arctic BC, SO₄, and PM₂.₅ concentration.
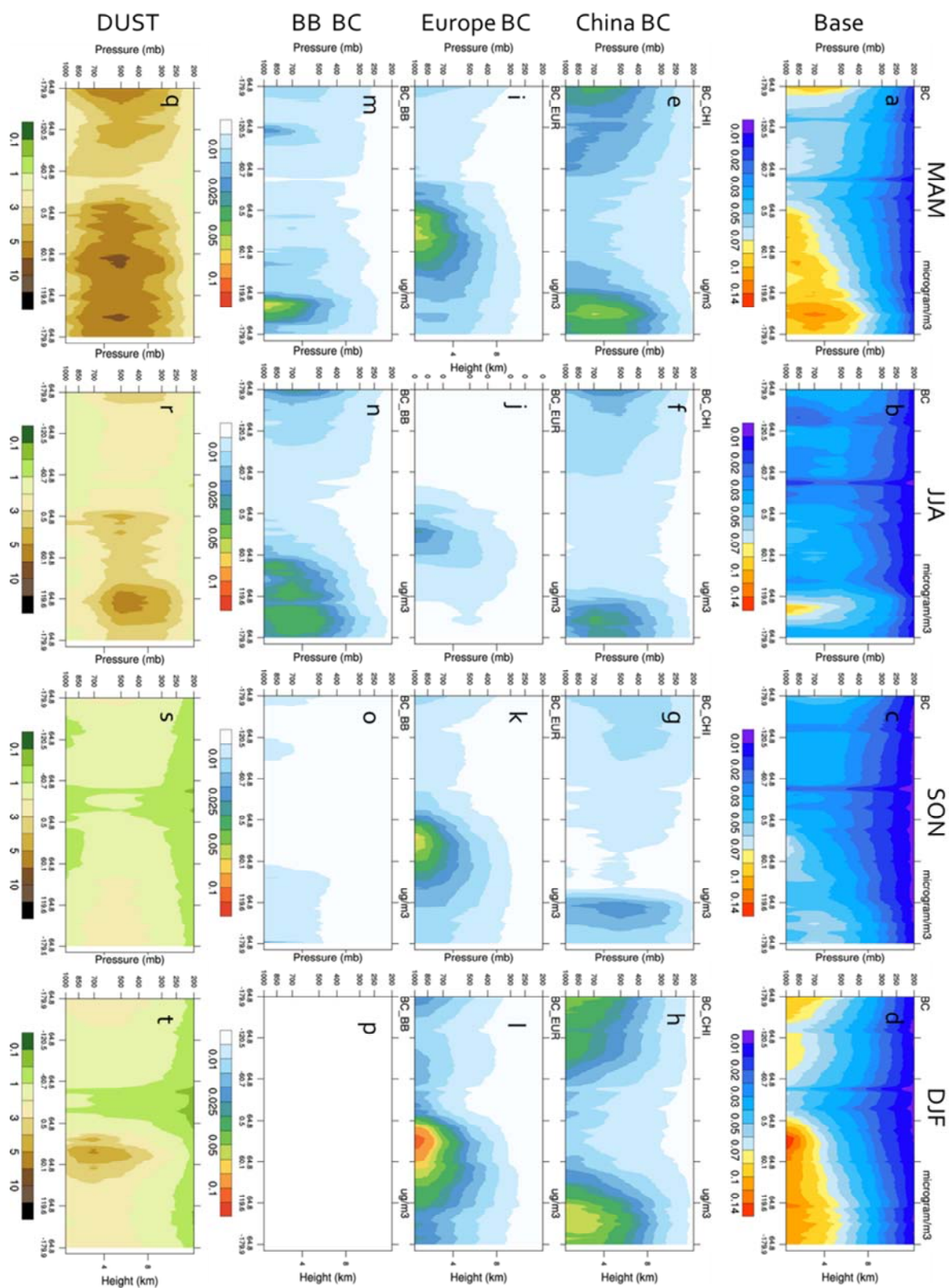
Figure 14: Cross-section at 64.8 °N for different seasons. The top and bottom rows show the BC and dust concentrations at the cross-section. The 2nd, 3rd and 4th rows show the contributions of China, Europe and biomass burning (BB) to BC at 64.8 °N.